Fractionation and Characterization of Petroleum Asphaltene: Focus on Metalopetroleomics

Fang Zheng [1,2], Quan Shi [2], Germain Salvato Vallverdu [1,3] [ID]**, Pierre Giusti [3,4]** [ID]
and Brice Bouyssiere [1,3,]* [ID]

[1] Institut des Sciences Analytiques et de Physico-Chimie pour l'Environnement et les Materiaux, Universite de Pau et des Pays de l'Adour, E2S UPPA, CNRS, IPREM, UMR5254, Hélioparc, 64053 Pau, France; zhengfangg@hotmail.com (F.Z.); germain.vallverdu@univ-pau.fr (G.S.V.)

[2] State Key Laboratory of Heavy Oil Processing, China University of Petroleum, Beijing 102249, China; sq@cup.edu.cn

[3] International Joint Laboratory C2MC, Complex Matrices Molecular Characterization, Total Research & Technology, Gonfreville, BP 27, F-76700 Harfleur, France; pierre.giusti@total.com

[4] Total Research & Technology, Gonfreville, BP 27, F-76700 Harfleur, France

* Correspondence: brice.bouyssiere@univ-pau.fr

Abstract: Asphaltenes, as the heaviest and most polar fraction of petroleum, have been characterized by various analytical techniques. A variety of fractionation methods have been carried out to separate asphaltenes into multiple subfractions for further investigation, and some of them have important reference significance. The goal of the current review article is to offer insight into the multitudinous analytical techniques and fractionation methods of asphaltene analysis, following an introduction with regard to the morphologies of metals and heteroatoms in asphaltenes, as well their functions on asphaltene aggregation. Learned lessons and suggestions on possible future work conclude the present review article.

Content

1. Introduction

Petroleum, as the most important source of energy and raw chemical materials, is a complex but delicately balanced system that depends on the relationship of its constituent fractions to each other [1]. Hence, the disturbance of these interactions, such as recovery and refining, may cause sediment formation and asphaltene deposition [2,3], which brings about many negative effects to the petroleum industry, such as the deactivation of catalysts, blocked pipelines, and deposition on the internal surface of the reservoirs [4–8].

Asphaltenes are the most polar fraction in crude oil, providing very low economic value and causing adverse effects to the oil industry. Images of n-heptane petroleum asphaltenes are shown in Figure 1. The content and characteristics of asphaltenes depend to a greater or lesser extent on the source of the crude oil [9]. Operationally, asphaltenes have up to now been defined as insoluble compounds in aliphatic hydrocarbons such as n-pentane or n-heptane, and soluble in aromatics such as toluene and benzene [10]. Asphaltenes are dark-brown-to-black friable solids that have no definite melting point, and usually foam and swell upon heating, leaving a carbonaceous residue [11]. The molecular weights of asphaltenes span a wide range, from hundreds to millions, leading to speculation about self-aggregation [12]. Carbon and hydrogen are the most abundant elements in asphaltenes, and the contents of carbon and hydrogen are usually greater than 90 wt%. These values correspond to a hydrogen-to-carbon atomic ratio of 1.15 in n-heptane (n-C7) asphaltenes [13]. In contrast to carbon and hydrogen, the content of undesired heteroatoms in asphaltenes usually greatly varies, especially sulfur [14]. Sulfur contents vary from 0.05 to 7.0 wt% [13]. On the other hand, the nitrogen content of asphaltene constituents has a somewhat lesser degree of variation (0.05–0.5 wt%), and oxygen contents generally less than 1.0 wt% [15]. In addition, there are some metallic elements in asphaltenes that are distributed in the range of 0–4000 ppm, among which nickel and vanadium are the most abundant. Metal atoms in asphaltenes are usually present in the form of metalloporphyrins [16], and as so-called "nonporphyrins", which has not been proved [17].

The composition and properties of asphaltenes have always been among the most important issues for petrochemistry. Over several decades, many researchers have contributed to the characterization, analysis, and determination of the physicochemical properties of asphaltenes with various analytical techniques, but these studies have only been partially successful, mainly because asphaltenes exhibit significant complexity. Asphaltene molecules are highly condensed and relatively high in undesired heteroatoms and metals, leading to stubborn self-aggregation [18]. Asphaltenes, defined as a solubility class, differ from a chemical class, so some variability among different asphaltenes is expected. To further

complicate the problem, multifarious differently sourced crude oils and preparation procedures exist for asphaltenes. The characterization of asphaltenes is still a very difficult and challenging issue.

Figure 1. Laboratory sample of asphaltenes extracted from crude oil in n-heptane (**left**) and n-pentane (**right**).

The object discussed in this paper is asphaltenes precipitated from crude oil or distillation residue rather than those from heavy fractions after chemical processing or coal.

2. Characterization Methods for Asphaltenes

2.1. Precipitation of Asphaltenes from Crude Oil

The precipitation and filtration of asphaltenes is generally carried out by using small molecules, *n*-alkanes. The procedure is performed with a variety of standard methods, as shown in Table 1. Each provides different results [19,20].

Table 1. Variety of asphaltene precipitation methods.

Method	Solvent	Solvent/Oil Ratio	Operating Conditions	Filter Media
ASTM D-3279-07	n-heptane	100:1	Reflux for 30 min, settle at ambient for 1 h, filter at 38–49 °C	Fiberglass, 1.5 μm
ASTM D-4124-01	n-heptane	100:1	Heat on steam bath for 30 min, settle at ambient overnight	Slow/medium paper, ~10 μm
ASTM D-4124-09	iso-octane	100:1	Reflux for 2 h, settle at ambient for 2 h	Medium glass frit, 10 μm
WRI	n-heptane	40:1	Heat to 80 °C for 5 min, stir at ambient for 16 h, settle for 30 min	Medium glass frit, 10 μm
ASTM D-6560-00	n-heptane	30:1	Reflux for 60 min, settle at ambient for 90–150 min	Whatman 42 paper, 2.5 μm
ASTM D-2007-03	n-pentane	10:1	Settle at ambient for 30 min	Rapid paper, 20 μm
IFP 9313 absorbance versus maltenes at 750 nm	n-heptane	20:1–200:1	Heat to 80 °C for 5 min, filter at ambient	Cellulose ester filter, 0.45 μm

2.2. Analytical Techniques for Asphaltene Properties

Asphaltenes, as the most mysterious fraction in petroleum, have had their properties studied for decades. The bulk properties of asphaltenes, such as element content, density, and thermogravimetric analysis, are nowadays well-known and can be readily determined via correlative analytical instruments [21,22]. A more comprehensive understanding of asphaltenes requires the utilization of specialized analysis methods. For example, Nuclear Magnetic Resonance (NMR) [23,24] and X-ray diffraction (XRD) [25] can be used to determine the average molecular parameters of asphaltenes. Vapor pressure osmometry (VPO), size exclusion chromatography (SEC), and mass spectrometry (MS) techniques can be used to measure the molecular weight distribution of asphaltenes [26–29].

In recent years, with its continuous development, MS technology and especially ultra-high-resolution (UHR) mass spectrometers are an indispensable tool for analyzing the chemical properties and molecular composition of asphaltenes [30–32]. Electrospray ionization (ESI) equipped Fourier transform ion cyclotron resonance–mass spectrometry (FT-ICR–MS) has long been used to characterize the molecular composition of asphaltenes, as early as a decade ago. ESI preferentially ionizes heteroatom-containing compounds such as polar N-, S-, O-, and metal-containing species. ESI FT-ICR–MS has been widely used to analyze the molecular composition of heteroatomic compounds in asphaltenes and their corresponding saturates, aromatics, and resins [33,34]. In addition, it is widely used in the research of petroleum porphyrin and geochemical porphyrin due to the good response of metalloporphyrins in ESI [35,36]. Compared to ESI, atmospheric-pressure photoionization (APPI) ionizes a wider range of compounds, including nonpolar compounds [37]. The APPI ionization source may obtain asphaltene-composition information not seen by ESI, such as polycyclic aromatic hydrocarbons (PAHs) [38]. Thus, APPI is widely used to characterize the molecular composition of petroleum asphaltenes and other components [39,40]. Although the resolution of Orbitrap is not as high as that of FT-ICR, its resolution ability cannot be ignored, and its stronger isolation and collision capabilities have unique advantages in studying the molecular composition and structural information of asphaltenes [41]. In addition, other ionization techniques (e.g., APCI, APLI, LDI, MALDI, and ASAP) equipped with ultra-high-resolution mass spectrometers are also applied to characterize asphaltenes [42–46].

Ultra-high-resolution mass spectrometers equipped with multiple ionization sources have an absolute advantage in the qualitative research of asphaltenes' molecular composition, but their quantitative results are affected by differences in ionization response and other substrates. Due to the limitations of molecular MS for the direct and quantitative identification of asphaltene compounds, inductively coupled plasma–high-resolution mass spectrometry (ICP–HR-MS) is an efficient tool for studying the size distribution of vanadium-, nickel-, and sulfur-containing compounds in asphaltenes. When ICP–MS is used to study asphaltenes, liquid chromatography (LC) is often used for online separation, and gel-permeation chromatography (GPC) is the most commonly used separation principle. The asphaltene solution (usually dissolved in tetrahydrofuran) is separated into high- (HMW), medium- (MMW), and low-molecular-weight (LMW) fractions after passing through GPC; then, it is analyzed online by mass spectrometry and simultaneously detected by UV or other detectors [47]. Despite criticisms of GPC, coupling GPC with ICP–MS allows for the identification and quantification of relative sizes associated with various V, Ni, and S compounds in asphaltenes [48]. Reinjected experiments revealed that the dissociation of asphaltene aggregates and reaggregation of LMW fractions occur after the isolation, as shown in Figure 2 [47].

Recently, high-resolution scanning probe microscopy has emerged as effective method for elucidating molecular structures, offering the unique capability of imaging a single adsorbate on the atomic scale. Attempts were made to use scanning tunneling microscopy (STM) to characterize asphaltenes, but no atomic resolution could be achieved on asphaltene molecules [49]. The latest advances in atomic force microscopy (AFM) enabled the direct observation of individual asphaltene molecules. Schuler et al. [50] studied more than 100 asphaltene molecules using AFM and STM, and provided the direct measurement of the tremendous range of molecular structures in asphaltenes. Images of asphaltene molecules derived from coal and petroleum are shown in Figure 3. This work is groundbreaking in the history of asphaltenes, allowing for us to have a direct visual understanding of the structure of some molecules in asphaltenes. This technique is also used to identify colloidal particles associated with asphaltene aggregates present in crude oils and the model system [51]. AFM even allows for direct observations on the specific structure of some biomarkers, such as the characterization of substitution patterns on petroporphyrins [52]. This technology constitutes a paradigm shift in the analysis of complex molecular mixtures, and may be applied to molecular electronics, organic light-emitting diodes, and photovoltaic devices [50].
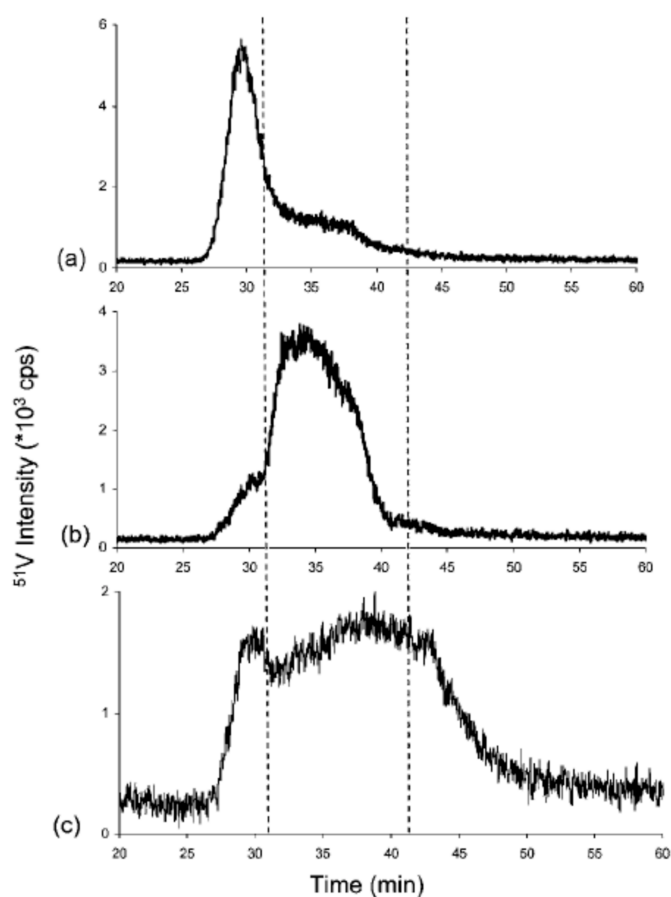
Figure 2. Chromatograms obtained by gel-permeation chromatography (GPC) inductively coupled plasma (ICP) MS of collected and reinjected (**a**) high-molecular-weight (HMW), (**b**) medium-molecular-weight (MMW), and (**c**) low-molecular-weight (LMW) fractions [47].
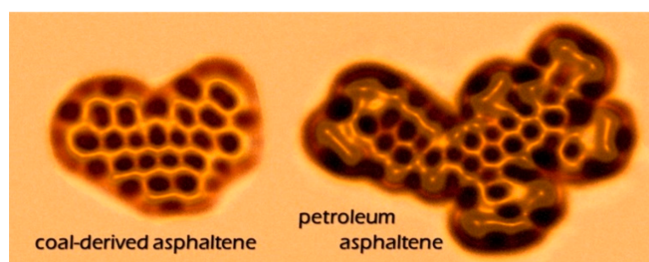
Figure 3. Atomic force microscopy (AFM) images of coal-derived asphaltenes and petroleum asphaltenes [50].

2.3. Analytical Techniques of Metal Content in Asphaltene

Petroleum is a complex mixture containing not only carbon, hydrogen, sulfur, oxygen, and nitrogen, but also many trace elements, including 45 metals, such as V, Ni, and Fe [53]. It is well-known that a fair amount of metal in crude oil exists in the asphaltene fraction. These metals are detrimental to petroleum processing, especially for accelerating catalyst deactivation [54]. Metal content is one of the important parameters for evaluating crude oil. Modern instrumental approaches to determine trace metals and asphaltenes in crude oil is by means of physical methods. Analytical methods were developed for the determination of metals in crude oils and derivatives using various analytical techniques, including flame atomic absorption spectrometry (FAAS) [55], graphite furnace atomic absorption spectrometry (GFAAS) [56], inductively coupled plasma optical-emission spectroscopy

(ICP–OES) [57], inductively coupled plasma–mass spectrometry (ICP–MS) [58], X-ray fluorescence spectroscopy [59], spectrophotometry [60], and high-performance liquid chromatography (HPLC) [61]. To date, concentrations of these metals in petroleum have mostly been determined by ICP–OES and ICP–MS because of their distinguished sensitivity, repeatability, and operability [62]. A large amount of data indicates that metal content in crude oil is between 1 and 10,000 μg/g, and concentrations of nickel and vanadium can reach up to several thousand ppm (*w/w*) [63]. The concentration of these metals in the asphaltene fraction is the most abundant. The concentration range of V, Ni, and Fe in asphaltenes from different studies is shown in Table 2.

Table 2. Concentrations of V, Ni, and Fe in asphaltenes with different origins.

Asphaltene Origin	Concentration Range of V (ppm)	Concentration Range of Ni (ppm)	Concentration Range of Fe (ppm)	Reference
Venezuela crude oil	1300–4000	300–410		[64]
Kuwait crude oil	200–800	50–120		[65]
Athabasca oil sand	640	240	260	[66]
Utah oil sand	21	170	4820	[66]
Russia Tatarstan crude oil	200–10,000	120–550		[67]
China Qingchuan gilsonite	3888	366	491	[68]
Texas shale	270	257	634	[36]

3. Asphaltene Fractionation

Instrumental analysis on asphaltenes is significant to obtain their physicochemical properties. Furthermore, combined with effective pretreatment, such as the fractionation of asphaltene, further information on the molecular composition is obtained. As asphaltene is the most complex component in petroleum, in order to more deeply study the physicochemical properties and structural composition of asphaltene, various studies attempted numerous methods to divide asphaltene into a series of narrow fractions, and comparatively analyzed their physical and chemical composition. Asphaltene itself is defined by solubility in solvents, that is, components in petroleum that are soluble in toluene or benzene, but insoluble in saturated hydrocarbons such as n-heptane. Asphaltenes are also "nondistillable" components, so the separation of asphaltenes is usually based on solubility. In addition, the separation of asphaltenes based on other physical and chemical methods is performed. With the development of analytical methods and technologies, even matrices as complex as asphaltenes could be separated with simple, effective, and rapid methods, and online fractionation methods have even emerged.

The separation of asphaltenes into fractions has two major advantages: It reduces the complexity of research materials and provides a property distribution rather than just averages. On the basis of the continuity model, this strategy was successfully applied to improve the characterization of asphaltenes, and it shows regular changes in the performance of different fractions. Generally, fractions with lower solubility show a decreased H/C ratio, and increased aromaticity and heteroatom content.

3.1. Sequential Elution Fractionation (SEF)

The solvent fractionation of petroleum and coal-related materials has been used to separate nondistillable fractions for more than 70 years. Generally, solvent fractionation requires Soxhlet extraction and repeated washing, which need several days of work. Boduszynski et al. [69]. Developed a faster and more robust method for solvent fractionation, originally used in research of solvent-refined coal. Later, this approach was successfully used to produce nondistillable petroleum fractions [70]. This method is sequential elution fractionation (SEF), and it involves the precipitation and dissolution of components in an inert column. Using this method, they demonstrated that nondistillable fractions followed the same patterns as those of distillation cuts, and that solubility could be used to perform equivalent distillation for nondistillable materials [71]. The SEF technique is based on

the principle of increasing the power of the used solvent to dissolve the sample. On the basis of the cohesive-parameter method, the solubility parameter of the fraction is expected to increase from the first eluted fraction (SF-1) to the last one (SF-6).

Generally, the SEF method requires petroleum or asphaltenes to first be loaded on the carrier and then eluted with different solvents. Here, the method of Rogel et al. [71] is taken as an example. A sample was deposited on 60 mesh nonporous polytetrafluoroethylene (PTFE) particles. After drying under nitrogen at room temperature, the PTFE-loaded sample was packed into a 35×2.83 cm cylindrical stainless-steel cell. The sample was extracted, with a sequence of solvents, at room temperature: heptane, 15/85 CH_2Cl_2/n-heptane, 30/70 CH_2Cl_2/n-heptane, 100% CH_2Cl_2, and 90/10 CH_2Cl_2/CH_3OH. This procedure generated four fractions: SF-1 (maltenes), and SF-2 to SF-5 (asphaltene fractions). Lastly, the cell was extracted three times with 90/10 CH_2Cl_2/CH_3OH at 120 °C for 15 min to obtain the last fraction (SF-6). Usually, this last fraction, SF-6, accounts for less than 0.5 wt% of the sample. This separation is compatible with the classical definition of maltenes as the soluble material in heptane, and asphaltenes as the insoluble one. After extractions, solvents were evaporated on a hot plate under a nitrogen atmosphere. Mass balance showed that the average recoveries were 90% to 99%.

Rogel et al. [72] separated Mexican vacuum residue asphaltenes and a thermally cracked residue using an automatic solvent extractor (ASE) apparatus. The characterization results showed the H/C ratio decreasing and aromaticity increasing with the solubility parameter of the solvent and the most polar asphaltene fractions having the highest concentrations of vanadium and nickel. They also fractionated asphaltene with the SEF method, and characterized physical and chemical properties on the basis of solubility [22]. High hydrogen deficiencies and uneven asphaltene component distribution were found to be the main factors causing asphaltene instability. Moreover, they found a strong relationship between larger aromaticity and stronger intermolecular force. LDI/APPI–FT-ICR–MS experiments suggested that H/C ratios and MWs were lower, and densities and solubility parameters were larger than those determined by other techniques. The preferentially ionized most aromatic molecules indicated that these techniques may be suitable for studying the most troublesome molecules in petroleum, which are less soluble and contain a heteroatomic functional group [73]. In addition, a deposit sample from an oilfield produced by CO_2 flooding was fractionated and compared with heptane asphaltenes extracted from the corresponding crude oil [21]. Results revealed that asphaltenes present in the deposit had lower solubility and higher aromaticity than those of heptane asphaltene extracted from crude oil, which suggested that heptane asphaltene may not be the best choice for the kinetic/thermodynamic modeling of this phenomenon. They also conducted APPI FT–ICR–MS analysis, and results showed that the field deposit contained more components with low aromaticity and more oxygen-containing species than heptane asphaltenes do. Conversely, heptane asphaltenes are rich in nitrogen-containing species [73].

This procedure was also performed by other studies using an n-heptane/toluene mixture to fractionate Boscan asphaltene at different temperature and contact time levels [74]. Characterization showed that the H/C ratio decreased, and aromaticity and N/C ratio increased with the aromaticity and polarity of the asphaltene fractions increasing. They found that asphaltenes acquired by precipitation had a higher molecular weight (tested by vapor-pressure infiltration (VPO)) than that of asphaltenes acquired by extraction.

The molecular weight distribution (MWD) of asphaltenes has been measured and controverted for decades. Various methods were used to test the molecular mass of asphaltenes, and values differ by as much as 10 times or more. VPO is a traditional method to measure the molecular weight of asphaltenes. Normally, values acquired from VPO are higher than those found with mass spectrometry (MS) techniques because VPO requires high analyte concentrations; in that case, asphaltene aggregation is known to occur [26]. Size-exclusion chromatography (SEC) could also obtain a higher asphaltene molecular weight value than that from MS due to the association phenomenon. However, a more precise average MW can be obtained when using calibration curves on the basis of chemicals that better mimic the chemical functionalities of real petroleum fractions instead of conventional polymer standards [27,75,76]. Fluorescence decay and depolarization were once used to

measure the molecular size and weight of asphaltenes by calibrating with known compounds [77,78]. However, conclusions derived from these techniques were found to be wrong because they were just sensitive to the fluorescent compounds, but asphaltene fluorescence is a highly complex function with unknown concentrations of different unknown components [79,80]. Laser desorption ionization (LDI) and/or matrix-assisted laser desorption ionization (MALDI) coupled with MS was also used to analyze the MWD of asphaltenes. The MWD of asphaltenes investigated by LDI–MS had monomer peaking at around 500 Da mass and a number-averaged WM of 800–1000 Da [28,29]. In 2008, Mullins, Marshall, et al. [81] published a comprehensive paper on asphaltenes' mass-weight distribution determined by four molecular-diffusion techniques and seven mass spectral techniques from many groups around the world. They concluded that all mass spectrometric measurements agree with all molecular diffusion methods, yield the same MWD for petroleum asphaltenes, and this range has an average molecular weight of ~750 Da (±200 Da) with a full width at half maxima (FWHM) of 500–1000 Da.

3.2. Solvent Extraction

The solvent fractionation of asphaltene is based on the equilibrium solubility of asphaltenes in the solution. Sequential elution can obtain a series of asphaltene fractions, but if the solvent is properly selected and supplemented by a valid physical or chemical treatment, asphaltenes can also be effectively separated by a single solvent-extraction step.

Miller and co-workers [82] separated asphaltenes into two fractions by extended Soxhlet extraction in n-heptane. The extracted fraction was noncolloidal, unassociated in aromatic solvents, while the unextracted fraction was colloidal, with higher apparent molecular weight and large aggregates in solution. The biggest difference between these two fractions was their degree of association in solution. Acevedo et al. [83] fractionated asphaltenes by complex formation with p-nitrophenol (PNP). PNP is known to generate charge transfer complexes with aromatic compounds, and it was recommended to form the same type of compound with asphaltene, leading to precipitation. Using this procedure, two asphaltene fractions (A_1 and A_2) with very different solubility were separated. Compared with low-soluble fraction A_1, the molecular weight (by VPO) of A_2 was lower, but the H/C mole was higher. Research results were used to propose a model for asphaltene colloidal solution in aromatic hydrocarbons in which low-soluble fraction A_1 would form a colloidal phase and dispersed in the media by soluble fraction A_2. The characterization of A_1 and A_2 showed that the low aromatic hydrogen and high H_α-type hydrogens in A_1 were consistent with a single, rigid, and flat core formed by the fusion of polycyclic aromatic and naphthenic units, while for A_2, high aromatic hydrogen and high H_α-type hydrogens corresponded with a more flexible structure where several smaller polycyclic aromatic and naphthenic units were joined by aliphatic chains [84]. Kilpatrick and co-workers [85] fractionated asphaltenes from four different crude oils with mixtures of heptane and toluene. The solubility profile results indicated strong cooperative asphaltene interactions of a particular subfraction, which was polar and hydrogen bonding. They found that this subfraction had the lowest H/C ratios and highest N, V, Ni, and Fe contents. They also found that the less soluble subfractions formed aggregates that were much larger than those of the more soluble subfractions.

Effective solvent extraction and separation can also be used to explore the morphotype of metal elements in asphaltenes. Gascon et al. [48] isolated asphaltenes with various solvents (methanol, acetic acid, acetonitrile, 1-propanol, acetone, methyl-tert-butyl-ether, ethyl acetate, acetylacetone, dimethylformamide, and diethylamine) and analyzed with GPC–ICP–MS. Results showed there were obvious differences in the apparent molecular weights of soluble and insoluble asphaltenes. They also established an optimized extraction procedure for the separation of the V, Ni, and S compounds present in asphaltenes.

3.3. Sequential Extraction

The sequential-extraction method performs continuous liquid–liquid extraction on asphaltenes. Compared with the SEF method, it does not require a loading step, but directly extracts. Two solvents are used as extractants in this method, and a series of asphaltene fractions are obtained on the basis of a charge of polarity of mixture compositions. Normally, a strong solvent (e.g., THF or toluene) and a normal paraffin (n-hexane or n-heptane) are chosen.

Acevedo et al. [86] divided asphaltene from Cerro Negro crude oil into seven extracts (F1–F7) and seven corresponding residues (R1–R7) as the THF–acetone mixture composition changed from 40% to 100% THF. The sample was placed in a Teflon membrane and attached to a flask device, placed in a Soxhlet apparatus, and extracted with boiling mixtures of acetone and THF. Result showed that the H/C ratio decreased, aromaticity increased, solubility decreased, and spin density increased with the increase in THF content. The last residues (R6 and R7) were found to be insoluble in organic solvents, indicating that these fractions were formed by molecular aggregates with strong intermolecular forces. Tojima et al. [87] used the toluene–heptane binary solvent system to fractionate nC_7-asphaltene precipitated from a Middle East vacuum residue into heavy and light fractions. The volume ratios of toluene/n-heptane for each separation step were 35/65, 25/75, and 18/82, respectively. They found that the lowest soluble fraction, defined as heavy asphaltene, consisted of the highest concentration of polynuclear aromatics. They also proposed a new conceptual model: Light asphaltenes would act as peptizing materials like resins, and heavy asphaltenes would be peptized in the oil. The same fractionation procedure was applied to Maya and Isthmus asphaltenes by Trejo et al. [88]. They conducted elemental, VPO, and NMR analysis on each fraction and found that the smallest fraction had more complex structures than those of other fractions. NMR methods [23,24] have proven to be extremely useful for defining the average molecular parameters of asphaltene fractions. Through the application of 1H-NMR [89–91], 13C-NMR [89,92–94], distorsionless enhancement by polarization transfer (DEPT) [95,96], solid-state (SS) NMR [94,97,98], and magnetic resonance imaging (MRI) [99–101], the hydrocarbon skeleton could be described in much detail. Although the chemical structure of asphaltene samples depends on geographical origin and even wells in the same crude oil production region, the deduced picture of asphaltenes from these studies is that of aromatic polycyclic clusters variably substituted with alkyl chains that may be quite long (up to C_{10}–C_{12}), and connected by alkyl and heteroatom bridges. The degree of condensation of each aromatic cluster may be more or less elevated, but generally does not exceed six rings [15].

This sequential-extraction method was also used to fractionated the hydrotreated products of Maya crude from different hydrotreated reaction conditions. Results of elemental analysis and MALDI–MS showed that the first fraction had the highest metal (Ni and V) content and lowest H/C ratio, indicating the presence of more aromatic asphaltenes [102]. Kharrat performed the sequential extraction of asphaltenes on the basis of a change of polarity of a binary system, THF, and n-hexane [103]. Asphaltene subfractions were separated by decreasing polarity of solvent mixtures, sequentially containing 30/70, 25/75, 20/80, 15/85, 10/90, 5/95, and 0/100 volumes of THF/hexane. Results from different analytical techniques indicated that the first fraction was more responsible for high viscosity, with a lower H/C ratio but higher metal, aromaticity, nitrogen, and sulfur contents, and highly condensed aromatic rings. This procedure can also be used to enrich metalloporphyrin in asphaltenes [39]. Asphaltene precipitated from Californian oil was further serially fractionated with solvent mixture toluene, 20:80 methanol/toluene, and 98:2 methanol/acetic acid. Nickel was enriched in the first fraction and further analyzed by APPI–FT-ICR–MS.

3.4. Column Chromatographic Fractionation

Column chromatography is an important method to study petroleum and its components, and it has been used to study petroleum asphaltenes for a long time. This work was initiated on chromatographic separations of asphaltenes in various chromatographic systems, adsorption on silica or clays [104,105], ion exchange [105,106], and gel-permeation chromatography (GPC) [107] to achieve

the gradual separation of asphaltenes. The adsorption method is based on the difference in component polarity; with increasing polarity and power of the solvent, that of the eluted fraction increased, and gradient separation was achieved [26]. Ion-exchange chromatography can divide asphaltenes into basic, acidic, and neutral (acid- and base-free asphaltenes) compounds. Some information on the chemical composition of asphaltenes can be obtained by comparing the behaviors of the three components. It is also meaningful to directly compare the behavior of acid- and base-free asphaltenes, and the original asphaltenes [106]. The fractionation of asphaltenes by GPC is based on their apparent molecular size with a powerful eluent such as THF [108]. GPC fractionation, combined with molecular weight measurements, can be used to study the association of asphaltenes and determine the true molecular weight of asphaltenes [109]. In less powerful solvents such as toluene and chloroform, incomplete asphaltene dissociation led to a high molecular weight. The asphaltenes fractions' molecular weights, determined in the most powerful solvent, dioxane-chloroform, were about 1050, suggesting that asphaltene molecules consisted of a number of unit sheets linked together rather than one large pericondensed aromatic ring system. GPC is also one of the methods to determine the molecular weight distribution of asphaltenes, and it was described in detail above.

The initial column chromatography separation method often used a larger column with an inner diameter of 2 cm and a length of about 100 cm. With the development of analytical techniques, small-volume chromatography columns combined with high-performance liquid chromatography (HPLC) have become the current mainstream. HPLC has several advantages. First, it provides the maximal number of fractions in the shortest time with less solvent consumption. Second, it offers repeatability, providing complete sample recovery. Third, it offers flexibility, as it can be momentarily adjusted and optimized. Fourth, it is easy to operate, with mild work-up procedures that avoid sample degradation [108].

HPLC equipped with GPC coupled to ICP–MS is effectively used to quantitatively study the existence of heteroatom- and metal-containing compounds in asphaltenes. Bouyssiere and his group have performed a lot of significant work in this area. They isolated asphaltenes into three fractions, HMW, MMW, and LMW. Reinjection experiments of the fractions revealed the association and dissociation behaviors of the asphaltene molecules [47]. The effect of different method parameters on the molecular size distribution of asphaltenes was also determined with GPC–ICP–MS. Aggregation asphaltenes were observed mainly during the first month; therefore, it is recommended that samples be prepared freshly for reproducible data [110].

Reversed-phase liquid chromatography has also been applied to the fractionation of asphaltenes using a cyanopropyl column with an optimized gradient from MeCN and water to NMP and THF [111]. A sample of 0.02 g/L asphaltenes was used, and three peaks, with two partially resolved, were evident in the fluorescence chromatogram. An extra weakly retained peak was detected by UV, but quenched fluorescence, suggesting asphaltene aggregation.

3.5. Sequential Precipitation

The process of sequential precipitation for fractionating asphaltene is the opposite of sequential extraction. A binary mixture of a "good" solvent (e.g., DCM and toluene) and a flocculent (usually paraffins, e.g., n-C_5 and n-C_7) is utilized. Total asphaltene is typically dispersed in a "good" solvent, and a flocculating solvent is added to induce partial precipitation. As the amount of flocculent is increased in the binary mixture, dissolving capacity decreases. Asphaltene fractions that precipitate out first are the more polar components, followed by precipitation of the less polar fractions upon the addition of more flocculent [112]. Specific procedures are diversified. A work done by Kilpatrick et al. [113] is very representative. Asphaltenes were expanded, isolated into 20–30 fractions by precipitation from mixtures of n-heptane and toluene. Upon the dissolution of asphaltene in toluene, n-heptane was added into the solution to induce partial precipitation of approximately 1%–2% of the whole asphaltene. The precipitated asphaltenes were isolated and recovered by filtration. The soluble fraction was dried and then dispersed in a mixture of a solvent containing a higher concentration of the flocculant, such that another 1%–2% of the whole asphaltene was precipitated.

The fractionation procedure continued using stepwise-increasing n-heptane as a flocculant until 20–30 fractions were isolated.

Another commonly used mixture solvent is DCM and n-C_5. Fogler and co-workers [114–116] fractionated asphaltenes into components with different polarities using binary mixtures of DCM and n-C5. In their program, the asphaltene fractions that precipitated first were the more polar fractions, followed by the precipitation of less polar fractions with the addition of more flocculent. Naphtha was also used as a "good" solvent using progressively more n-heptane as a flocculating solvent to isolate asphaltene into several fractions [117].

Chemical composition and structure analysis on the fractions with various types of equipment usually follows the fractionation procedure. The first subfraction to precipitate was that with the most polarity and aromaticity, with the highest concentration of metals. The atomic H/C ratio systematically increased, and the metalloporphyrin contents were observed to decrease as fractionation proceeded. The more polar fraction had a lower H/C ratio, and a higher content of heteroatoms and metals (i.e., V, Ni, and Fe) than those of less polar fractions [114]. The subfraction of asphaltenes with the largest average size and the highest aromaticity also had the strongest tendency to aggregate [113].

3.6. On-Column Method

The previously discussed methods, extensive and time-consuming experimental methodologies, were developed to fractionate asphaltenes. The on-column method, developed by Schabron et al. [19,118], is a faster and simpler fractionation procedure to separate asphaltenes into solubility fractions using asphaltene precipitation and redissolution. In this procedure, a sample of crude oil or its asphaltenes is injected into a polytetrafluoroethylene (PTFE)-packed column using n-heptane as carrier solvent. Once asphaltenes are precipitated on the column, and maltenes are eluted, the solvent is first shifted to cyclohexane, followed by toluene, and lastly to DCM. Fractions can be quantified using an evaporative light-scattering detector (ELSD). This method requires a small amount of the sample and takes less than 30 min to determine, and can quantify asphaltene contents as low as 120 ppm with good repeatability and reproducibility. Meaningfully, it can be automated and be used online [119].

This new solvent system was improved by Ovalles et al. [72], making the on-column methodology more robust and repeatable. They used mixtures of heptane, DCM, and methanol in an attempt to make changes in solubility parameters quantifiable and gradual. This modified procedure was successfully applied to the characterization of processed samples, and they found that low-solubility-parameter asphaltenes were easy to react [72]. They also used a filter instead of a PTFE column for the determination of asphaltene content. Results showed that the use of a filter was a significant advancement in the reliability of asphaltene testing with low-flow operating rates, making it possible to couple the asphaltene separation with other techniques such as GPC, MS, and ICP [120].

3.7. Ultracentrifugation

Ultracentrifugation is carried out to separate asphaltene dissolving in toluene into six fractions depending on different asphaltene mass. The structure of these fractions was analyzed using viscosity and X-ray scattering [121]. The mass densities showed very small differences between all asphaltene fractions. However, the mass of the smallest and largest asphaltene aggregates differed by two decades, indicating that the separation of asphaltenes using ultracentrifugation depends on different mass rather than different density. They also found that asphaltenes formed nanometric aggregates but did not overlap [122].

X-ray and neutron-scattering techniques are usually to extract geometrical parameters of asphaltene nanoaggregates in a good solvent, such as overall size, particle volume, polydispersity, internal structure, and surface properties (e.g., rough or smooth) [25,123]. However, these techniques conventionally fail to assess > 50 nm structures, with a severe limitation existing for the study of insoluble asphaltenes. Image analysis of optical micrographs also provides structural insight for length scales > 500 nm. Recently, ultra-small-angle X-ray scattering (USAXS) was applied to characterize the size and morphology of

asphaltene precipitation systems. USAXS allows for researchers to probe the size and structure of asphaltenes spanning 1 nm to 5 μm with a time resolution on the order of minutes. This technique covers the gap in the characterization capabilities of asphaltenes over the length scales between 50 and 500 nm, which has potentially severe consequences [124]. Yang et al. [125] monitored the process of asphaltenes precipitating with USAXS for the first time, and results revealed that asphaltenes precipitating in a heptane−toluene mixture show a hierarchical structure of an asphaltene-rich phase and further agglomerate into fractal flocs. In addition, the size and concentration of soluble asphaltenes do not change during precipitation, whereas the structure of insoluble asphaltenes varies. Yang et al. [126] also studied the effect of chemical inhibitors on asphaltene precipitation and morphology using USAXS.

X-ray diffraction (XRD) has been employed to obtain structural information of asphaltene, evaluating the interplay between aromatic sheets of asphaltene molecules and providing the dimensions of the molecules. XRD studies on a large number of asphaltenes showed that their aromaticity is in the range of 0.21–0.51, with a stacking number between five and eight [25]. XRD gives quantitative intensity curves, and structural parameters can be obtained from the shape and position of the peaks [127]. However, as reported by Andersen et al. [128], determining the crystallographic parameters of asphaltenes is on the basis of many assumptions and the data processing method. In interpreting the data, special care must be taken to oversimplify very complex asphaltene systems. Sacking is only one type of asphaltene aggregates, and more complex association schemes must be considered.

3.8. Supercritical Fluid Extraction (SFE)

Supercritical fluid extraction (SFE) is the process of separating one component from the matrix using supercritical fluids as the extracting solvent. Carbon dioxide (CO_2) is the most used supercritical fluid, sometimes modified by co-solvents. Extraction conditions for supercritical fluids are above the critical temperature and critical pressure. Upon this, the supercritical fluid has the dual characteristics of gas and liquid, with a strong penetration force, similar to the gas, and high density and solubility, similar to the liquid. SFE was performed on asphaltene using CO_2 as solvent under various experimental conditions. The extracts, up to 12% of the whole asphaltenes, contained alkanes, aromatics, and polar compounds [129]. The supercritical fluid extraction fractionation (SFEF) procedure was developed for the deep and clean separation of heavy hydrocarbons with low-carbon-number alkanes (e.g., propane, butane, and pentane) as supercritical solvents [130]. SFEF was usually devoted to separating heavy oils, residues, and oil sands. Afterwards, various aspects of narrow SFEF subfractions were investigated, such as hindered diffusion, solubility parameters, information on alkyl side chains, average structure, and molecular composition [131].

3.9. Ultrafiltration Fractionation

Membrane filtration was used to reduce asphaltene size polydispersity, and gain insight into asphaltene properties [132,133]. Results showed that asphaltene aggregates of different sizes can be fractionated by membrane filtration in a more selective way compared with using solvent flocculation. The driving force involved in asphaltene diffusion through porous membranes is the concentration gradient, implementing their size segregation. Small asphaltene aggregates have lower aromaticity and higher aliphatic composition, with shorter alkyl chains, compared with large aggregates.

3.10. Adsorption onto Porous Medium

Recently, a new fractionation procedure was developed on the basis of the adsorption of asphaltenes onto a porous medium, $CaCO_3$. Three asphaltene fractions were obtained: the bulk (non-adsorbed) asphaltene that stayed in the bulk solution, the adsorbed asphaltene that was obtained by desorption of asphaltenes adsorbed on $CaCO_3$ using tetrahydrofuran, and the irreversibly adsorbed asphaltene that was obtained after $CaCO_3$ dissolution [134–136]. The irreversibly adsorbed fraction, containing the highest concentration of carbonyl, carboxylic acid, or derivative groups was found to have a significantly higher tendency to self-associate and form larger aggregates than other fractions did, which exhibited

similar properties with the fraction precipitating first from the sequential precipitation procedure [135]. The effect of these three asphaltene fractions on wax crystallization was also studied, and results showed that the irreversibly adsorbed fraction containing the most polar species induced the largest changes in wax-crystal morphology [136].

Fractionation experiments of asphaltenes deposited in other porous mediums, such as silica, calcite, dolomite, and sandstone, were also carried out [4,137]. Asphaltenes were fractionated into four fractions, bulk, normally adsorbed, hard-adsorbed, and irreversibly adsorbed, with a Soxhlet extraction step added before dissolving the calcium carbonate [137–139]. A new experimental model of asphaltene deposition was developed on the basis of the deposition analysis of these asphaltene fractions in porous media under dynamic conditions, which resulted in good correlation for the asphaltene classifications in the porosity and permeability reduction model [138,139].

3.11. Microwave Treatment

The microwave electromagnetic field could promote molecular motion extremely well, which presents its effectiveness in asphaltene fractionation [140]. An asphaltene solution could be rapidly separated into soluble and insoluble fractions with microwave irradiation, and it was diluted by a polar solvent. Vanadyl porphyrins were released and enriched in the soluble fraction, presenting stronger characteristic absorption in UV–vis. This may become an alternative way to purify petroporphyrins from crude oils and asphaltenes.

The fractionation of asphaltenes is a critical procedure for asphaltene pretreatment. Moreover, combining this procedure and efficient analytical techniques can lead to a better understanding of the physicochemical properties of asphaltenes.

4. Characterization of Heteroatoms and Metals in Asphaltenes

Petroleum asphaltenes are predominantly composed of hydrogen and carbon, typically in amounts greater than 90%. ^{13}C NMR and X-ray studies show that carbon distribution is typically about 40% aromatic and the remainder is saturated [141]. However, hydrogen is found primarily (>90%) on saturated carbons, predominantly methylene groups, as determined by Fourier transform infrared (FT-IR) and NMR spectroscopy [141]. FT-IR spectroscopy has long been used to determine the types and relative contents of functional groups in asphaltenes with different origins, which offers information on the aromatic and alkyl carbon fractions, and pinpoints polydispersity in the chemical composition of asphaltene with hydrogen-to-carbon atom ratio in the range of 1–1.3 [142]. X-ray diffraction studies indicated that asphaltenes possess a few stacked layers of condensed aromatic ring systems [15]. ^{13}C NMR and FT-IR results indicated that these ring systems contain alicyclic and alkyl substituents [141]. These spectroscopic results can be analyzed, further yielding a detailed picture of the distribution of carbon and hydrogen in asphaltenes. By combining results from a variety of methods, chemical structures are suggested that are expected to be close to actual asphaltene molecular structures for the distribution of carbon and hydrogen [15]. However, the quantification of contained heteroatoms and metals is more problematic [14]. Asphaltenes generally contain small quantities of heteroatoms and metals, amounting to a few percentage points. Heteroatomic chemical functions are often polar and sometimes charged, yielding strong intermolecular interactions. Metal atoms could be complexed by heteroatoms, bringing diverse and adverse impact on petroleum refinement. Thus, understanding heteroatomic chemistry and metal morphology is an essential component of asphaltene characterization.

4.1. Sulfur in Asphaltenes

Sulfur is the most abundant heteroatom in petroleum, generally ranging from 0.05 to 7.0 wt% [143]. Crude oils made from them vary in sulfur content according to origin. Sulfur-containing compounds in crude oils can be categorized into six basic types in terms of their functional groups: H_2S, elemental sulfur, mercaptans, sulfides, thiophenes, and polysulfides. Sulfones and sulfoxides are also in small

quantities in many crude oils and mainly remain in asphaltene fraction. These oxidized sulfur species are generated through oxidation in reservoirs by contact with oxic water or by subsequent extraction when exposed to air [15]. Total sulfur in crude oil and its fractions can be determined by X-ray fluorescence (XRF), ICP–OES, AAS, and ICP–MS [144].

Sulfur-containing compounds are responsible for the corrosive character and poisoning of catalysts in petroleum refining. Polluting atmospheric gases, produced by petroleum product combustion, contribute to the formation of acid rain, causing serious environmental damage [145]. The speciation and quantification of sulfur-containing compounds in petroleum and its fractions are very significative. Sulfur-containing compounds in light petroleum fractions can be practicably separated and enriched for chemical structure determination. Analysis of sulfur-containing compounds in asphaltene fractions is more challenging because of their complexity and matrix effects.

X-ray absorption near-edge structure spectroscopy (XANES) offers a powerful and nondestructive technique for the identification and quantification of chemical structure heteroatoms in asphaltenes [146]. Deconvolution is usually conducted on XANES spectra to improve resolution and dissolve the mixtures [15]. The results of sulfur XANES on asphaltenes showed that thiophene is the most dominant functional, generally followed by sulfide [15,147,148]. Sulfoxides are the most dominant form of the oxidized sulfur species, but they are not found in all samples. Thiophene sulfone was also detected in some asphaltene samples by derivative XANES spectra [149]. These oxidized sulfur compounds are related to the special reservoir environment, or may be oxidized during transportation and storage.

GPC–ICP–HR-MS was applied to separate and monitor the size distribution of sulfur-containing compounds in asphaltenes and other petroleum fractions [48,64,150]. Sulfur-containing compounds are predominant in aromatics and resins (75%–90%), and only 10%–25% are distributed in asphaltenes, indicating that medium polarity is prominent [64]. Sulfur compounds present in asphaltenes are mainly associated with the high-molecular-weight fraction (70%–80%) [48].

The molecular composition of heteroatom-containing species in asphaltenes was analyzed by FT-ICR–MS. Molecular formulas of these polar compounds can be directly observed with the high resolution of the ICR. Multi-hetero-atomic sulfur-containing compounds such as N_1S_1, O_1S_1, S_2, and S_3 species were detected in asphaltenes [151–153]. Sulfur-containing vanadyl porphyrins in petroleum asphaltenes were also identified by APPI–FT-ICR–MS [154]. High-resolution mass spectrometry possesses unique advantages in analyzing heteroatom-containing compounds in complex matrices.

4.2. Nitrogen in Asphaltenes

The content of nitrogen element in petroleum is generally 0.05–0.5 wt%, with an obvious increase in nitrogen concentrations in vacuum bottoms and asphaltenes [15]. Nitrogen XANES studies on asphaltenes demonstrated that almost all nitrogen found in asphaltenes is aromatic, existing in pyrrolic or pyridinic form. Pyrrolic nitrogen is more predominant than pyridinic forms are. Contributions from (saturated and aromatic) amines were found to be negligible [147].

High-resolution mass spectrometry provides a molecular level understanding of the existence of nitrogen-containing compounds in asphaltenes [155]. The most abundant N_1 class species in Venezuela asphaltenes is dibenzocarbazoles [151]. DBE values of N_1 class species are all above 9, which means that these compounds have higher aromaticity than that of carbazole and phenanthridine. A similar DBE distribution of N_1 class species also exists in the asphaltene fractions of Liaohe crude oil and Canadian oil-sand bitumen [33,152]. The highest relative abundance of N_1 class species in Liaohe asphaltene was at a DBE of 9, 12, 15, and 18 for carbazoles, benzocarbazoles, dibenzocarbazoles, and benzonaphthocarbazoles, respectively [33]. Thus, arylcarbazole should be the predominant form of N_1 class species. Multi-hetero-atomic nitrogen-containing compounds are also widely distributed in asphaltenes, and all perform a high degree of condensation.

The porphyrin compound in asphaltene is also a kind of nitrogen-containing compound, and its existence form is described in detail below.

4.3. Oxygen in Asphaltenes

Oxygen-containing compounds in petroleum can generally be categorized into two types according to their acidic–basic properties: acidic compounds, mainly composed of phenol and carboxylic acid, which is usually referred to as petroleum acid; and neutral compounds, mainly containing aldehydes, ethers, esters, and furans. Oxygen in asphaltenes is primarily present in the form of a phenolic hydroxyl function, contributing strong hydrogen bonding for intermolecular association [156,157]. Infrared spectroscopic examination on asphaltenes indicated that two or more oxygen-containing functions (hydroxyl and carbonyl) may reside in the same aromatic ring or a condensed aromatic system [158]. Recent studies indicated that higher-order oxygen-containing compounds contain lower abundance-weighted DBE values, suggesting that lower aromaticity is offset by higher oxygen content [159]. These low-condensation molecules with high oxygen content residing in the asphaltene fraction may be due to hydrogen bonding. The morphology of oxygen-containing compounds in asphaltenes is more complicated than that of nitrogen and sulfur species because there are further oxygen-containing functional groups, and hydrogen bonding performs a crucial role in the aggregation behavior of petroleum asphaltenes.

4.4. Metals in Asphaltenes

The most abundant and troublesome metal-containing compounds present in petroleum deposits are vanadium and nickel. The majority of these complexes are contained within the highly aromatic, highly polar asphaltene fraction, posing significant difficulties [17,54]. The exact molecular form of these metals remains the focus of controversy among researchers in the field. An undoubted fact is that a portion of vanadium and nickel in asphaltene deposits is in the form of petroporphyrins [35,36]. These compounds are derived from chlorophylls and hemes (hemoglobins) in living organisms [160,161].

UV–vis is widely used in the identification and quantification of petroporphyrins because of the sensitive electronic absorption [162]. However, the measured UV–vis absorption of petroporphyrins is much too small to account for the total vanadium and nickel content in asphaltenes, that is, a significant part of the porphyrins presents in the asphaltene fraction, lacking this characteristic absorption [163]. Therefore, the "nonporphyrin" definition was introduced. However, no corroborated "nonporphyrin" compound has been found to date [17]. The bonding structure surrounding vanadium and nickel atoms within the asphaltenes determined by EXAFS and XANES showed that all of them present in asphaltene samples are present as a metal ion (i.e., V = O and Ni) coordinated to four nitrogen ligands [164–167]. A major barrier to the effective quantitation of petroporphyrins in asphaltene is the significant interference from asphaltene matrix [168]. The lack of characteristic porphyrin absorption in asphaltenes could be attributed to the chemical interactions between asphaltene and porphyrin molecules [169].

4.5. Metals in Asphaltene by MS Molecular Technique

Most available analytical techniques, such as elementary, X-ray, and NMR methods, give bulk and/or average properties, but little detailed information on a molecular level. The structural information of some porphyrin molecules could be obtained by means of HT-GC–MS [170]. Asphaltene molecules were characterized by pyrolysis-HT GC–MS, in which asphaltenes were pyrolyzed by using a CDS pyroprobe at a temperature of 610 °C. Molecular characterization by this technique in asphaltenes represents another challenge: Are these compounds part of the asphaltene structure or are they simply trapped in the asphaltenes during precipitation [171]? Similar obstacles exist in characterizing metal-containing compounds with HT-GC–MS due to the strong aggregation between them and asphaltene molecules.

The emergence of high-resolution mass spectrometry technology led to new developments in the characterization of petroporphyrins [172,173]. The highest mass accuracy of FT-ICR MS improves analysis for identifying trace polar compounds within asphaltenes. Mckenna et al. [172],

and Qian et al. [39] identified vanadyl and nickel porphyrins in heavy crude oil and asphaltene by atmospheric-pressure photoionization (APPI) FT-ICR–MS combined with offline chromatographic fractionation. Qian et al. [154] gave primary evidence of sulfur-containing vanadyl porphyrins in petroleum asphaltene. Zhao et al. [35] combined chromatographic fractionation with ESI–FT-ICR–MS, and identified three series of vanadyl porphyrins that contained functional oxygen groups. Shi et al. [36] detected simultaneous vanadyl, nickel, iron, and gallium porphyrins in an asphaltene sample derived from marine shale with ESI–FT-ICR–MS. An overview of known vanadyl, nickel, and iron petroporphyrin types is shown in Table 3 [174].

Table 3. Overview of known vanadyl, nickel, and iron petroporphyrin types.

	Vanadyl Porphyrins	Nickel Porphyrins	Iron Porphyrins	Reference
Multioxygen	$C_mH_nN_4VO_1$	$C_mH_nN_4Ni$	$C_mH_nN_4Fe$	[36]
	$C_mH_nN_4VO_2$	$C_mH_nN_4NiO_1$	$C_mH_nN_4FeO_1$	[36]
	$C_mH_nN_4VO_3$		$C_mH_nN_4FeO_2$	[36]
	$C_mH_nN_4VO_4$			[35]
Multisulfur	$C_mH_nN_4VO_1S_1$			[154]
	$C_mH_nN_4VO_1S_2$			[174]
	$C_mH_nN_4VO_1S_3$			[174]
Multinitrogen	$C_mH_nN_5VO_1$			[175]
Multi-hetero-atomic	$C_mH_nN_4VO_2S_1$			[174]
	$C_mH_nN_4VO_3S_1$			[174]
	$C_mH_nN_4VO_4S_1$			[174]
	$C_mH_nN_4VO_2S_2$			[174]
	$C_mH_nN_4VO_3S_2$			[174]
	$C_mH_nN_5VO_2$			[175]
			$C_mH_nN_5FeO_2$	[36]

4.6. Metals in Asphaltene by Inorganic Techniques

Determination of metal content showed that discrete asphaltene fractions with lower solubility have higher metal concentrations [113]. The contents of metal elements in these fractions are usually determined by ICP–OES or ICP–MS. Moreover, the size distributions of metals in asphaltenes could be well characterized by GPC–ICP–MS [110]. Approximately 80% of total V present in HMW and MMW compounds is in nanoaggregate form. HMW compounds were even observed in an asphaltene solution that was diluted by 40,000-fold (25 mg/kg), indicating that the interaction between asphaltene molecules is strong enough to resist the dissolution/dilution factor of the solvent [64]. Other metals in asphaltene, such as sodium and calcium, are presumed to exist in the form of organic carboxylates. However, so far, their presence has not been confirmed due to the complexity of asphaltenes.

The characterization of metal-containing compounds by using gas chromatography with a high-temperature injector and an atomic emission detector (HT-GC–AED) provides valuable information on identification of metal porphyrin species in heavy oil fractions and asphaltenes [65,176]. Although most V-containing compounds in the asphaltenes are nonvolatile and cannot be analyzed by GC even with high temperatures, these results revealed that porphyrin units exist in the asphaltenes, linked to larger aggregates [65]. V and the Ni complexes present in asphaltene fractions display a strong interaction with their matrices.

5. Metals and Heteroatoms Involved in Asphaltene Aggregation

Molecular aggregation is a common phenomenon encountered in many chemical and biochemical systems because of strong association interactions between molecules [177]. The size distribution of aggregate asphaltenes span a range of 1000–100,000 g/mol in apparent molecular weight, with leading physical dimensions of 2–20 nm [178]. Driving forces contributing to aggregations include π–π stacking (electrostatic and/or van der Waals forces) [179], hydrogen bonding [113], acid-base interactions [180],

and coordination interactions [181]. These aggregates are suspended and stable in most unmodified crude oils and aromatic solvents such as toluene [182]. Asphaltene deposition emerges when pressure [183], temperature [184], composition, and shear rate [2,185] change, which is responsible for operational problems related to well production and exploration [186], oil transportation, oil refining and processing, and emulsion stabilization [6,7,187]. It is generally acknowledged that asphaltene fractions aggregate to form nanoparticles and clusters throughout a range of concentration and temperature [188]. Aggregation of asphaltenes occurs even in exceptionally diluted solutions. These aggregates dissociate with the decrease in concentration and increase in temperature [189,190]. In addition, metals and heteroatoms play an important role in asphaltene aggregation [113,191].

5.1. Asphaltene Aggregate Morphologies

Petroleum chemists have paid much attention to the morphological study of asphaltene aggregates for a long time [18,192]. Various morphologies were proposed with mathematical functions and approximation models, such as colloidal/micellar, polymeric, solubility, and modified Yen models [193]. With considerable consensus in various studies on the molecular structure of asphaltene aggregates, the modified Yen model was concluded to be the most suitable representation of aggregated asphaltenes [191]. The Yen model was proposed by Professor Ten Fu Yen and co-workers in 1967, accounting for chemical moieties in asphaltenes [194] This model, modified by Mullins et al. [188] (2010), specifies the dominant molecular and colloidal structure of asphaltenes, and it is called the modified Yen model (also known as the Yen–Mullins model). Figure 4 shows a graphical representation of this model, with asphaltene molecules being able to form asphaltene nanoaggregates with fewer than six aggregation numbers [188,195]. In this model, the basic force of aggregation comes from the attraction between the large aromatic cores of asphaltene molecules. Steric hindrance driven by peripheral substituents limits the molecular numbers of association. The interior attractive force and exterior repulsive force of asphaltene molecules lead to a low molecule number of nanoaggregate particles. These nanoaggregates can form asphaltene clusters. These clusters (less than 10 nm) were not much larger than nanoaggregates were, and quite smaller than flocs, which are on the micron scale [196]. Asphaltene clusters are likely fractal in their scaling, with much smaller binding energy compared with that of nanoaggregate binding [121]. The modified Yen model shows considerable consistency with later experiment results [191]. This model provides a convincible definition for the nano- and cluster aggregation of asphaltene molecules. Nevertheless, recent studies indicated that asphaltenes form primary aggregates at concentrations as low as ca. 0.7 mg/L, which is far below the value advocated by the modified Yen model [190].

Figure 4. Modified Yen model [195].
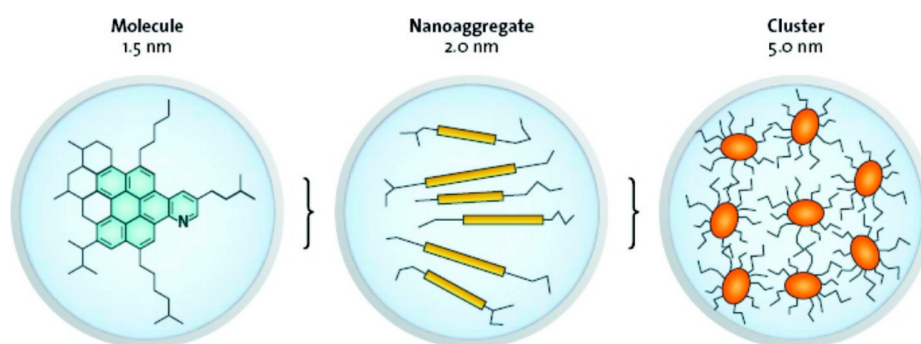
Another model of asphaltene aggregates was proposed by Murray R. Gray et al. [179]. They suggested that the general motifs of supramolecular assembly observed in simple mixtures are related to asphaltene aggregation, and the stoichiometry and thermodynamics of aggregation in complex petroleum mixtures. There is no strong donor–acceptor interaction in petroleum, but large asphaltene molecules

produce multiple cooperative associations that combine acid-base interactions, hydrogen bonding, metal coordination, hydrophobic pockets, and aromatic π–π stacks. They considered the known chemistry of petroleum and the canonical properties of asphaltene fractions. Schematic representation of the supramolecular assembly of this model is shown in Figure 5.

Figure 5. Supramolecular assembly model of asphaltene proposed by Murray R. Gray et al. [179].

5.2. Methods on Asphaltene Aggregates

In order to confirm the reason and mechanism of asphaltene aggregation, numerous experimental methods were implemented, as well as molecular simulations that can be classified into three routes:

(i) Conventional route (i.e., direct approach) [197]: fractionation of whole asphaltenes into several subfractions, independently investigating these fractions to monitor the aggregation of asphaltenes with various analytical methods and instruments. The studies of asphaltene fractions by a sequential precipitation procedure showed that the earliest precipitation contains most inorganic solids and the last fraction, similar in chemical composition and aggregation behavior to that of petroleum resins. Interactions of petroporphyrins also appear to play a key role in the asphaltene aggregation mechanism [113]. A comparable conclusion was drawn by other researchers to observe the structure and dispersion of petroleum asphaltene aggregates. This indicates that most polar fractions, insoluble in organic solvents such as heptane, are formed by nanoaggregates of molecules held in place by strong intermolecular forces [86].

(ii) Model compound route [198]: Asphaltene model compounds with known physicochemical properties are used to mirror asphaltene architecture. In order to study the association behavior due to the polyfunctional nature of asphaltenes, a series of pyrene derivative compounds, including hydroxyl groups, ketone alkyl side chains, and alkyl bridges, were synthesized and characterized, using methods such as vapor-pressure osmometry and neutron scattering [199]. It was inferred that nonpolar pyrene and derivatives had no relevance with asphaltene self-aggregation behavior, while polar functional groups (ketones and hydroxyls) gave stronger association of pyrene-based compounds in solution. Later investigations using 4,4′-bis-(2-pyren-1-yl-ethyl)-[2,2′]bipyridinyl (PBP) as a model compound found that the occurrence of aggregation was at the same concentration range as that of asphaltene in solution, with an average molecular weight of 500–700 Da. They also found that the self-aggregation of PBP was due to π–π stacking interactions, including both pyrene rings and the bipyridine spacer [200]. Another series of model

compounds, alkyl hexabenzocoronene (HBC) derivatives, was also synthesized to investigate the self-aggregation behavior of asphaltene in solution. This showed that both alkyl–alkyl and π–π stacking interactions are responsible for spontaneous aggregation behavior [201].

(iii) Molecular simulation route [202,203]: the utilization of computational chemistry and molecular simulations studies to investigate aggregation behavior. The complex chemical configuration of asphaltene makes it difficult to obtain a portion of information on molecular structure and dynamics, while molecular simulation can obtain information on the molecular level, so as to corroborate the correctness of the theory within an ideal state setting. In addition, the correlation between the structure and properties of the research object can be confirmed by experimental simulation. Atomistically detailed models and molecular dynamics simulations were applied to investigate the aggregation of asphaltene molecules in solution [204]. It was inferred that the solubility parameter of the asphaltene aggregate decreased with the increase in aggregation number, and more stable dimers were obtained with an increase in the ratio of n-heptane to toluene. These results were in good agreement with experimental evidence [205]. Other methodologies were implemented to investigate the aggregation behavior of asphaltene molecules such as density functional theory (DFT) [206]. From the screening of various model compounds it was concluded from molecular dynamics simulations or DFT calculations that hydrogen bonding is as much important as π–π stacking interactions to drive the asphaltene aggregation [207].

5.3. Role of Heteroatoms and Metals in Asphaltene Aggregation

Heteroatoms in asphaltene, in the form of polar functional groups, inevitably unbalance the charge density, inducing permanent or partial dipoles that do not exist in nonpolar fractions. Sulfur atoms present as sulfides and thiophenes in asphaltenes increase the condensation extent of asphaltene molecules, and sulfide bridged bonds could expand the size of asphaltene molecules. Nevertheless, sulfur-containing groups are only slightly polar and seem to have no contribution to intermolecular aggregation [113]. Unlike sulfur-, oxygen-, and nitrogen-containing function groups in asphaltenes are generally polar and competent in participating in strong intermolecular aggregation. Nitrogen atoms in pyrrolic and pyridinic forms, and oxygen present as phenolic and carboxylic acid are responsible for hydrogen bond accepter and donor species [191]. Polycyclic compounds containing pyridine functional groups were investigated to study the influence of both aromatic and aliphatic parts of asphaltene molecules on their aggregation via determining association free energies. Heteroatoms residing in the aromatic core significantly affected the interaction strength more than ones connected to the aliphatic side chains. Heteroatoms dwelling in the polycyclic core could impact electronic cloud density, which alters associative strength [208]. Nitrogen and oxygen are more electronegative than carbon is, which can enhance electrostatic attraction in both isolated and solvent environments, leading to the aggregation of asphaltenes via hydrogen bonds [112,209]. The interactions of metalloporphyrins concentrated in the asphaltene fraction appear to play a pivotal role in the aggregation of asphaltenes [113].

Molecular simulation methods provide an efficient way to explore the role of metalloporphyrins in asphaltene aggregation at the atomic scale. The investigation of asphaltene aggregation via a molecular simulation route should consider both the thermodynamic conditions [210,211] and chemical compositions [210,212,213] of the system. The competition between π-stacking interactions due to the aromaticity and the formation of hydrogen bonds due to the presence of heteroatoms demonstrated that the presence of hydrogen bonds is a key factor for the formation of large aggregates [213]. The presence of H bonds between porphyrins and asphaltenes by polar lateral chains can enhance π–π interactions, an about twofold increase [213]. The π-stacking interactions are not strong enough to explain why porphyrins are commonly found within asphaltene aggregates [214]. The formation and stabilization of asphaltene nanoaggregates are dependent on the size of the conjugated core and the eventual presence of polar groups capable of forming H bonds [212,215]. Vanadyl porphyrins, even without polar lateral chains, can interact considerably strongly with asphaltene molecules via the formation of H bonds from the central O atom [194,213].

6. Conclusions and Prospective

The fractionation of asphaltene is important for the better understanding of its composition and properties, which reduces its complexity and provides property distribution rather than just averages. Effective analytical techniques play a vital role in the determination of physicochemical properties of asphaltenes, which are defined as a solubility class presenting the most polar fraction of petroleum, in which contents of heteroatoms and metals are very high. The presence of these undesirable elements is responsible for abundant polar functional groups. Driving forces contributing to aggregations not only include interactions between aromatic cores, but are also supplied by interactions among these polar functional groups. Asphaltene aggregation and deposition cause severe problems to the oil industry, causing catalyst deactivation, blocking pipelines, and causing deposition on the internal surface of the reservoirs. A comprehensive understanding of the chemical structure and aggregation mechanism of asphaltene has always been one of the most important issues for petrochemistry. To further complicate the matter, a variety of different source materials and preparation procedures exists for asphaltenes. Hence, accredited fractionation procedures and analytical techniques are essential. In spite of various morphologies having been proposed with mathematical functions and approximation models, the modified Yen model is the most suitable representation of aggregated asphaltenes, providing a convincible definition for nano and cluster aggregation of asphaltene molecules. New knowledge emerges as technology advances and research progresses. Key factors of future research are threefold:

- The initial sample: The first creation of "standard" asphaltene samples, Asphaltene 2017 [216], was a first good point in order to focus all available analytical techniques on the same sample because, most of the time, results on asphaltene cannot be compared because they were obtained with different samples. This first tentative asphaltene reference material should be reproduced in the future.
- Fractionation should consider the "petrointeractomic" aspect, and try to keep intact nanoaggregates that are present in crude oil for further characterization.
- Molecular modelization might have an important role in understanding nanoagreggation, and for that, all heteroatoms and metals that can be present in asphaltenes should be considered.

This situation is what we expected, and it should contribute to the success of more advanced fractionation/analytical techniques in which high-resolution mass spectrometry and spectroscopy may be the key to solving these asphaltene problems. Furthermore, the increase in calculation capacity can, in the near future, authorize us to build aggregation models near the reality of identified asphaltene molecules.

Conflicts of Interest: The authors declare no conflict of interest.

References

1. Chilingarian, G.V.; Yen, T.F. *Bitumens, Asphalts, and Tar Sands*; Elsevier: Amsterdam, The Netherlands, 1978.
2. Hong, E.; Watkinson, P. A study of asphaltene solubility and precipitation. *Fuel* **2004**, *83*, 1881–1887. [CrossRef]
3. Enayat, S.; Rajan Babu, N.; Kuang, J.; Rezaee, S.; Lu, H.; Tavakkoli, M.; Wang, J.; Vargas, F.M. On the development of experimental methods to determine the rates of asphaltene precipitation, aggregation, and deposition. *Fuel* **2020**, *260*, 116250. [CrossRef]

4.   Nascimento, P.T.H.; Santos, A.F.; Yamamoto, C.I.; Tose, L.V.; Barros, E.V.; Gonçalves, G.R.; Freitas, J.C.C.; Vaz, B.G.; Romão, W.; Scheer, A.P. Fractionation of Asphaltene by Adsorption onto Silica and Chemical Characterization by Atmospheric Pressure Photoionization Fourier Transform Ion Cyclotron Resonance Mass Spectrometry, Fourier Transform Infrared Spectroscopy Coupled to Attenuated Total Reflectance, and Proton Nuclear Magnetic Resonance. *Energy Fuels* **2016**, *30*, 5439–5448. [CrossRef]

5.   Speight, J.G. Petroleum Asphaltenes—Part 2: The Effect of Asphaltene and Resin Constituents on Recovery and Refining Processes. *Oil Gas Sci. Technol.* **2004**, *59*, 479–488. [CrossRef]

6.   Akbarzadeh, K.; Hammami, A.; Kharrat, A.; Zhang, D.; Allenson, S.; Creek, J.; Kabir, S.; Jamaluddin, A.; Marshall, A.G.; Rodgers, R.P. Asphaltenes—Problematic but rich in potential. *Oilfield Rev.* **2007**, *19*, 22–43.

7.   Ribeiro, F.S.; Souza Mendes, P.R.; Braga, S.L. Obstruction of pipelines due to paraffin deposition during the flow of crude oils. *Int. J. Heat Mass Transf.* **1997**, *40*, 4319–4328. [CrossRef]

8.   Ok, S.; Mal, T.K. NMR Spectroscopy Analysis of Asphaltenes. *Energy Fuels* **2019**, *33*, 10391–10414. [CrossRef]

9.   Wen, C.S.; Chilingarian, G.; Yen, T.F. Properties and structure of bitumens. In *Bitumens, Asphalts and Tar Sands*; Elsevier: Amsterdam, The Netherlands, 1978; Volume 7, pp. 155–190.

10.   Speight, J.G. Petroleum Asphaltenes—Part 1: Asphaltenes, Resins and the Structure of Petroleum. *Oil Gas Sci. Technol.* **2004**, *59*, 467–477. [CrossRef]

11.   Mullins, O.C.; Sheu, E.Y. *Structures and Dynamics of Asphaltenes*; Springer Science and Business Media: New York, NY, USA, 2013.

12.   Badre, S.; Carla Goncalves, C.; Norinaga, K.; Gustavson, G.; Mullins, O.C. Molecular size and weight of asphaltene and asphaltene solubility fractions from coals, crude oils and bitumen. *Fuel* **2006**, *85*, 1–11. [CrossRef]

13.   Mullins, O.C.; Sheu, E.Y.; Hammami, A.; Marshall, A.G. *Asphaltenes, Heavy Oils, and Petroleomics*; Springer Science and Business Media: New York, NY, USA, 2007.

14.   Simanzhenkov, V.; Idem, R. *Crude Oil Chemistry*; CRC Press: Boca Raton, FL, USA, 2003.

15.   Sheu, E.Y.; Mullins, O.C. *Fundamentals and Applications*; Springer: New York, NY, USA, 1995.

16.   Yen, T.F.; Chilingarian, G.V. *Asphaltenes and Asphalts, 2: Part B*; Elsevier: Amsterdam, The Netherlands, 2000.

17.   Dechaine, G.P.; Gray, M.R. Chemistry and Association of Vanadium Compounds in Heavy Oil and Bitumen, and Implications for Their Selective Removal. *Energy Fuels* **2010**, *24*, 2795–2808. [CrossRef]

18.   Vargas, F.M.; Tavakkoli, M. *Asphaltene Deposition: Fundamentals, Prediction, Prevention, and Remediation*; CRC Press: Boca Raton, FL, USA, 2018.

19.   Schabron, J.F.; Rovani, J.F.; Sanderson, M.M. Asphaltene Determinator Method for Automated On-Column Precipitation and Redissolution of Pericondensed Aromatic Asphaltene Components. *Energy Fuels* **2010**, *24*, 5984–5996. [CrossRef]

20.   Kharrat, A.M.; Zacharia, J.; Cherian, V.J.; Anyatonwu, A. Issues with Comparing SARA Methodologies. *Energy Fuels* **2007**, *21*, 3618–3621. [CrossRef]

21.   Rogel, E.; Miao, T.; Vien, J.; Roye, M. Comparing asphaltenes: Deposit versus crude oil. *Fuel* **2015**, *147*, 155–160. [CrossRef]

22.   Rogel, E.; Roye, M.; Vien, J.; Miao, T. Characterization of Asphaltene Fractions: Distribution, Chemical Characteristics, and Solubility Behavior. *Energy Fuels* **2015**, *29*, 2143–2152. [CrossRef]

23.   Brown, J. A Study of the Hydrogen Distribution in Coal-like Materials by High-resolution Nuclear Magnetic Resonance Spectroscopy I-The Measurement and Interpreatation of the Spectra. *Fuel* **1960**, *39*, 79–86.

24.   Brown, J.; Ladner, W. A study of the hydrogen distribution in coal-like materials by high-resolution nuclear magnetic resonance spectroscopy. 2. A comparison with infra-red measurement and the conversion to carbon structure. *Fuel* **1960**, *39*, 87–96.

25.   Eyssautier, J.; Levitz, P.; Espinat, D.; Jestin, J.; Gummel, J.; Grillo, I.; Barré, L. Insight into Asphaltene Nanoaggregate Structure Inferred by Small Angle Neutron and X-ray Scattering. *J. Phys. Chem. B* **2011**, *115*, 6827–6837. [CrossRef]

26.   Strausz, O.P.; Peng, P.A.; Murgich, J. Ab5out the Colloidal Nature of Asphaltenes and the MW of Covalent Monomeric Units. *Energy Fuels* **2002**, *16*, 809–822. [CrossRef]

27.   Guzman, A.; Bueno, A.; Carbognani, L. Molecular Weight Determination of Asphaltenes from Colombian Crudes by Size Exclusion Chromatography (SEC) and Vapor Pressure Osmometry (VPO). *Pet. Sci. Technol.* **2009**, *27*, 801–816. [CrossRef]

28. Hortal, A.R.; Martínez-Haya, B.; Lobato, M.D.; Pedrosa, J.M.; Lago, S. On the determination of molecular weight distributions of asphaltenes and their aggregates in laser desorption ionization experiments. *J. Mass Spectrom.* **2006**, *41*, 960–968. [CrossRef]

29. Martínez-Haya, B.; Hortal, A.R.; Hurtado, P.; Lobato, M.D.; Pedrosa, J.M. Laser desorption/ionization determination of molecular weight distributions of polyaromatic carbonaceous compounds and their aggregates. *J. Mass Spectrom.* **2007**, *42*, 701–713. [CrossRef] [PubMed]

30. Marshall, A.G.; Rodgers, R.P. Petroleomics: The Next Grand Challenge for Chemical Analysis. *Acc. Chem. Res.* **2004**, *37*, 53–59. [CrossRef] [PubMed]

31. Rodgers, R.P.; Marshall, A.G. Petroleomics: Advanced Characterization of Petroleum-Derived Materials by Fourier Transform Ion Cyclotron Resonance Mass Spectrometry (FT-ICR MS). In *Asphaltenes, Heavy Oils, and Petroleomics*; Mullins, O.C., Sheu, E.Y., Hammami, A., Marshall, A.G., Eds.; Springer: New York, NY, USA, 2007; pp. 63–93. [CrossRef]

32. Marshall, A.G.; Rodgers, R.P. Petroleomics: Chemistry of the underworld. *Proc. Natl. Acad. Sci. USA* **2008**, *105*, 18090. [CrossRef] [PubMed]

33. Shi, Q.; Hou, D.; Chung, K.H.; Xu, C.; Zhao, S.; Zhang, Y. Characterization of Heteroatom Compounds in a Crude Oil and Its Saturates, Aromatics, Resins, and Asphaltenes (SARA) and Non-basic Nitrogen Fractions Analyzed by Negative-Ion Electrospray Ionization Fourier Transform Ion Cyclotron Resonance Mass Spectrometry. *Energy Fuels* **2010**, *24*, 2545–2553. [CrossRef]

34. Klein, G.C.; Kim, S.; Rodgers, R.P.; Marshall, A.G.; Yen, A. Mass Spectral Analysis of Asphaltenes. II. Detailed Compositional Comparison of Asphaltenes Deposit to Its Crude Oil Counterpart for Two Geographically Different Crude Oils by ESI FT-ICR MS. *Energy Fuels* **2006**, *20*, 1973–1979. [CrossRef]

35. Xu, Z.; Yu, L.; Xu, C.; Yan, Y.; Zhang, Y.; Zhang, Q.; Zhao, S.; Chung, K.; Gray, M.R.; Quan, S. Separation and Characterization of Vanadyl Porphyrins in Venezuela Orinoco Heavy Crude Oil. *Energy Fuels* **2013**, *27*, 2874–2882.

36. Zheng, F.; Hsu, C.S.; Zhang, Y.; Sun, Y.; Wu, Y.; Lu, H.; Sun, X.; Shi, Q. Simultaneous Detection of Vanadyl, Nickel, Iron, and Gallium Porphyrins in Marine Shales from the Eagle Ford Formation, South Texas. *Energy Fuels* **2018**, *32*, 10382–10390. [CrossRef]

37. Huba, A.K.; Huba, K.; Gardinali, P.R. Understanding the atmospheric pressure ionization of petroleum components: The effects of size, structure, and presence of heteroatoms. *Sci. Total Environ.* **2016**, *568*, 1018–1025. [CrossRef]

38. Jiang, B.; Liang, Y.; Xu, C.; Zhang, J.; Hu, M.; Shi, Q. Polycyclic Aromatic Hydrocarbons (PAHs) in Ambient Aerosols from Beijing: Characterization of Low Volatile PAHs by Positive-Ion Atmospheric Pressure Photoionization (APPI) Coupled with Fourier Transform Ion Cyclotron Resonance. *Environ. Sci. Technol.* **2014**, *48*, 4716–4723. [CrossRef]

39. Qian, K.; Edwards, K.E.; Mennito, A.S.; Walters, C.C.; Kushnerick, J.D. Enrichment, Resolution, and Identification of Nickel Porphyrins in Petroleum Asphaltene by Cyclograph Separation and Atmospheric Pressure Photoionization Fourier Transform Ion Cyclotron Resonance Mass Spectrometry. *Anal. Chem.* **2010**, *82*, 413–419. [CrossRef]

40. McKenna, A.M.; Chacón-Patiño, M.L.; Weisbrod, C.R.; Blakney, G.T.; Rodgers, R.P. Molecular-Level Characterization of Asphaltenes Isolated from Distillation Cuts. *Energy Fuels* **2019**, *33*, 2018–2029. [CrossRef]

41. Nyadong, L.; Lai, J.; Thompsen, C.; LaFrancois, C.J.; Cai, X.; Song, C.; Wang, J.; Wang, W. High-Field Orbitrap Mass Spectrometry and Tandem Mass Spectrometry for Molecular Characterization of Asphaltenes. *Energy Fuels* **2018**, *32*, 294–305. [CrossRef]

42. Lozano, D.C.P.; Thomas, M.J.; Jones, H.E.; Barrow, M.P. Petroleomics: Tools, Challenges, and Developments. *Annu. Rev. Anal. Chem.* **2020**. [CrossRef] [PubMed]

43. Panda, S.K.; Brockmann, K.-J.; Benter, T.; Schrader, W. Atmospheric pressure laser ionization (APLI) coupled with Fourier transform ion cyclotron resonance mass spectrometry applied to petroleum samples analysis: Comparison with electrospray ionization and atmospheric pressure photoionization methods. *Rapid Commun. Mass Spectrom.* **2011**, *25*, 2317–2326. [CrossRef] [PubMed]

44. Gaspar, A.; Zellermann, E.; Lababidi, S.; Reece, J.; Schrader, W. Characterization of Saturates, Aromatics, Resins, and Asphaltenes Heavy Crude Oil Fractions by Atmospheric Pressure Laser Ionization Fourier Transform Ion Cyclotron Resonance Mass Spectrometry. *Energy Fuels* **2012**, *26*, 3481–3487. [CrossRef]

45. Witt, M.; Godejohann, M.; Oltmanns, S.; Moir, M.; Rogel, E. Characterization of Asphaltenes Precipitated at Different Solvent Power Conditions Using Atmospheric Pressure Photoionization (APPI) and Laser Desorption Ionization (LDI) Coupled to Fourier Transform Ion Cyclotron Resonance Mass Spectrometry (FT-ICR MS). *Energy Fuels* **2018**, *32*, 2653–2660. [CrossRef]

46. Pereira, T.M.C.; Vanini, G.; Tose, L.V.; Cardoso, F.M.R.; Fleming, F.P.; Rosa, P.T.V.; Thompson, C.J.; Castro, E.V.R.; Vaz, B.G.; Romão, W. FT-ICR MS analysis of asphaltenes: Asphaltenes go in, fullerenes come out. *Fuel* **2014**, *131*, 49–58. [CrossRef]

47. Caumette, G.; Lienemann, C.P.; Merdrignac, I.; Bouyssiere, B.; Lobinski, R. Fractionation and speciation of nickel and vanadium in crude oils by size exclusion chromatography-ICP MS and normal phase HPLC-ICP MS. *J. Anal. At. Spectrom.* **2010**, *25*, 1123–1129. [CrossRef]

48. Gascon, G.; Negrín, J.; Montoto, V.G.; Acevedo, S.; Lienemann, C.-P.; Bouyssiere, B. Simplification of Heavy Matrices by Liquid–Solid Extraction: Part II—How to Separate the LMW, MMW, and HMW Compounds in Asphaltene Fractions for V, Ni, and S Compounds. *Energy Fuels* **2019**, *33*, 8110–8117. [CrossRef]

49. Watson, B.A.; Barteau, M.A. Imaging of Petroleum Asphaltenes Using Scanning Tunneling Microscopy. *Ind. Eng. Chem. Res.* **1994**, *33*, 2358–2363. [CrossRef]

50. Schuler, B.; Meyer, G.; Peña, D.; Mullins, O.C.; Gross, L. Unraveling the Molecular Structures of Asphaltenes by Atomic Force Microscopy. *J. Am. Chem. Soc.* **2015**, *137*, 9870–9876. [CrossRef] [PubMed]

51. Balestrin, L.B.d.S.; Cardoso, M.B.; Loh, W. Using Atomic Force Microscopy to Detect Asphaltene Colloidal Particles in Crude Oils. *Energy Fuels* **2017**, *31*, 3738–3746. [CrossRef]

52. Zhang, Y.; Schulz, F.; Rytting, B.M.; Walters, C.C.; Kaiser, K.; Metz, J.N.; Harper, M.R.; Merchant, S.S.; Mennito, A.S.; Qian, K.; et al. Elucidating the Geometric Substitution of Petroporphyrins by Spectroscopic Analysis and Atomic Force Microscopy Molecular Imaging. *Energy Fuels* **2019**, *33*, 6088–6097. [CrossRef] [PubMed]

53. Liang, W. *Petroleum Chemistry*, 2nd ed.; China University of Petroleum Press: Beijing, China, 2009.

54. Elliot, J.D. *Delayed Coker Design and Operation: Recent Trends and Innovations*; Foster Wheeler USA Corporation: Clinton, NJ, USA, 1996.

55. Guidroz, J.M.; Sneddon, J. Fate of vanadium determined by nitrous oxide–acetylene flame atomic absorption spectrometry in unburned and burned Venezuelan crude oil. *Microchem. J.* **2002**, *73*, 363–366. [CrossRef]

56. Aucélio, R.Q.; Doyle, A.; Pizzorno, B.S.; Tristão, M.L.B.; Campos, R.C. Electrothermal atomic absorption spectrometric method for the determination of vanadium in diesel and asphaltene prepared as detergentless microemulsions. *Microchem. J.* **2004**, *78*, 21–26. [CrossRef]

57. De Souza, R.M.; Meliande, A.L.S.; da Silveira, C.L.P.; Aucélio, R.Q. Determination of Mo, Zn, Cd, Ti, Ni, V, Fe, Mn, Cr and Co in crude oil using inductively coupled plasma optical emission spectrometry and sample introduction as detergentless microemulsions. *Microchem. J.* **2006**, *82*, 137–141. [CrossRef]

58. Duyck, C.; Miekeley, N.; Porto da Silveira, C.L.; Szatmari, P. Trace element determination in crude oil and its fractions by inductively coupled plasma mass spectrometry using ultrasonic nebulization of toluene solutions. *Spectrochim. Acta Part B At. Spectrosc.* **2002**, *57*, 1979–1990. [CrossRef]

59. Iwasaki, K.; Tanaka, K. Preconcentration and x-ray fluorescence: Determination of vanadium, nickel and iron in residual fuel oils and in particulate material from oil-fired sources. *Anal. Chim. Acta* **1982**, *136*, 293–299. [CrossRef]

60. Mastoi, G.M.; Khuhawar, M.Y.; Bozdar, R.B. Spectrophotometric determination of vanadium in crude oil. *J. Quant. Spectrosc. Radiat. Transf.* **2006**, *102*, 236–240. [CrossRef]

61. Khuhawar, M.Y.; Arain, G.M. Liquid chromatographic determination of vanadium in petroleum oils and mineral ore samples using 2-acetylpyridne-4-phenyl-3-thiosemicarbazone as derivatizing reagent. *Talanta* **2006**, *68*, 535–541. [CrossRef]

62. López, L.; Lo Mónaco, S. Geochemical implications of trace elements and sulfur in the saturate, aromatic and resin fractions of crude oil from the Mara and Mara Oeste fields, Venezuela. *Fuel* **2004**, *83*, 365–374. [CrossRef]

63. Yen, T.F. *Role of Trace Metals in Petroleum*; Ann Arbor Science Publishers: Ann Arbor, MI, USA, 1975.

64. Gascon, G.; Vargas, V.; Feo, L.; Castellano, O.; Castillo, J.; Giusti, P.; Acevedo, S.; Lienemann, C.-P.; Bouyssiere, B. Size Distributions of Sulfur, Vanadium, and Nickel Compounds in Crude Oils, Residues, and Their Saturate, Aromatic, Resin, and Asphaltene Fractions Determined by Gel Permeation Chromatography Inductively Coupled Plasma High-Resolution Mass Spectrometry. *Energy Fuels* **2017**, *31*, 7783–7788. [CrossRef]

65. Park, J.-I.; Al-Mutairi, A.; Marafie, A.M.J.; Yoon, S.-H.; Mochida, I.; Ma, X. The characterization of metal complexes in typical Kuwait atmospheric residues using both GPC coupled with ICP–MS and HT GC–AED. *J. Ind. Eng. Chem.* **2016**, *34*, 204–212. [CrossRef]

66. Kotlyar, L.S.; Ripmeester, J.A.; Sparks, B.D.; Woods, J. Comparative study of organic matter derived from Utah and Athabasca oil sands. *Fuel* **1988**, *67*, 1529–1535. [CrossRef]

67. Yakubov, M.R.; Sinyashin, K.O.; Abilova, G.R.; Tazeeva, E.G.; Milordov, D.V.; Yakubova, S.G.; Borisov, D.N.; Gryaznov, P.I.; Mironov, N.A.; Borisova, Y.Y. Differentiation of heavy oils according to the vanadium and nickel content in asphaltenes and resins. *Pet. Chem.* **2017**, *57*, 849–854. [CrossRef]

68. Zheng, F.; Zhu, G.-Y.; Chen, Z.-Q.; Zhao, Q.-L.; Shi, Q. Molecular composition of vanadyl porphyrins in the gilsonite. *J. Fuel Chem. Technol.* **2020**, *48*, 562–567. [CrossRef]

69. Boduszynski, M.M.; Hurtubise, R.J.; Silver, H.F. Separation of solvent-refined coal into solvent-derived fractions. *Anal. Chem.* **1982**, *54*, 372–375. [CrossRef]

70. Boduszynski, M.M. Composition of heavy petroleums. 1. Molecular weight, hydrogen deficiency, and heteroatom concentration as a function of atmospheric equivalent boiling point up to 1400.degree.F (760 °C). *Energy Fuels* **1987**, *1*, 2–11. [CrossRef]

71. Rogel, E.; Roye, M.; Vien, J.; Witt, M. Equivalent Distillation: A Path to a Better Understanding of Asphaltene Characteristics and Behavior. In *The Boduszynski Continuum: Contributions to the Understanding of the Molecular Composition of Petroleum*; American Chemical Society: Washington, DC, USA, 2018; Volume 1282, pp. 51–72.

72. Ovalles, C.; Rogel, E.; Moir, M.; Thomas, L.; Pradhan, A. Characterization of Heavy Crude Oils, Their Fractions, and Hydrovisbroken Products by the Asphaltene Solubility Fraction Method. *Energy Fuels* **2012**, *26*, 549–556. [CrossRef]

73. Rogel, E.; Witt, M. Atmospheric Pressure Photoionization Coupled to Fourier Transform Ion Cyclotron Resonance Mass Spectrometry to Characterize Asphaltene Deposit Solubility Fractions: Comparison to Bulk Properties. *Energy Fuels* **2016**, *30*, 915–923. [CrossRef]

74. Andersen, S.I.; Keul, A.; Stenby, E. Variation in Composition of Subfractions of Petroleum Asphaltenes. *Pet. Sci. Technol.* **1997**, *15*, 611–645. [CrossRef]

75. Nali, M.; Manclossi, A. Size exclusion chromatography and vapor pressure osmometry in the determination of asphaltene molecular weight. *Fuel Sci. Technol. Int.* **1995**, *13*, 1051–1264. [CrossRef]

76. Sato, S.; Takanohashi, T.; Tanaka, R. Molecular Weight Calibration of Asphaltenes Using Gel Permeation Chromatography/Mass Spectrometry. *Energy Fuels* **2005**, *19*, 1991–1994. [CrossRef]

77. Groenzin, H.; Mullins, O.C. Asphaltene Molecular Size and Structure. *J. Phys. Chem. A* **1999**, *103*, 11237–11245. [CrossRef]

78. Groenzin, H.; Mullins, O.C. Molecular Size and Structure of Asphaltenes from Various Sources. *Energy Fuels* **2000**, *14*, 677–684. [CrossRef]

79. Strausz, O.P.; Safarik, I.; Lown, E.M.; Morales-Izquierdo, A. A Critique of Asphaltene Fluorescence Decay and Depolarization-Based Claims about Molecular Weight and Molecular Architecture. *Energy Fuels* **2008**, *22*, 1156–1166. [CrossRef]

80. Morgan, T.J.; Millan, M.; Behrouzi, M.; Herod, A.A.; Kandiyoti, R. On the Limitations of UV−Fluorescence Spectroscopy in the Detection of High-Mass Hydrocarbon Molecules. *Energy Fuels* **2005**, *19*, 164–169. [CrossRef]

81. Mullins, O.C.; Martínez-Haya, B.; Marshall, A.G. Contrasting Perspective on Asphaltene Molecular Weight. This Comment vs the Overview of A.A. Herod, K.D. Bartle, and R. Kandiyoti. *Energy Fuels* **2008**, *22*, 1765–1773. [CrossRef]

82. Miller, J.T.; Fisher, R.B.; Thiyagarajan, P.; Winans, R.E.; Hunt, J.E. Subfractionation and Characterization of Mayan Asphaltene. *Energy Fuels* **1998**, *12*, 1290–1298. [CrossRef]

83. Gutiérrez, L.B.; Ranaudo, M.A.; Méndez, B.; Acevedo, S. Fractionation of Asphaltene by Complex Formation with p-Nitrophenol. A Method for Structural Studies and Stability of Asphaltene Colloids. *Energy Fuels* **2001**, *15*, 624–628. [CrossRef]

84. Acevedo, S.; Escobar, O.; Echevarria, L.; Gutiérrez, L.B.; Méndez, B. Structural Analysis of Soluble and Insoluble Fractions of Asphaltenes Isolated Using the PNP Method. Relation between Asphaltene Structure and Solubility. *Energy Fuels* **2004**, *18*, 305–311. [CrossRef]

85. Spiecker, P.M.; Gawrys, K.L.; Kilpatrick, P.K. Aggregation and solubility behavior of asphaltenes and their subfractions. *J. Colloid Interface Sci.* **2003**, *267*, 178–193. [CrossRef]

86. Acevedo, S.; Escobar, G.; Ranaudo, M.A.; Piñate, J.; Amorín, A.; Díaz, M.; Silva, P. Observations about the Structure and Dispersion of Petroleum Asphaltenes Aggregates Obtained from Dialysis Fractionation and Characterization. *Energy Fuels* **1997**, *11*, 774–778. [CrossRef]

87. Tojima, M.; Suhara, S.; Imamura, M.; Furuta, A. Effect of heavy asphaltene on stability of residual oil. *Catal. Today* **1998**, *43*, 347–351. [CrossRef]

88. Trejo, F.; Centeno, G.; Ancheyta, J. Precipitation, fractionation and characterization of asphaltenes from heavy and light crude oils. *Fuel* **2004**, *83*, 2169–2175. [CrossRef]

89. Dutta Majumdar, R.; Gerken, M.; Mikula, R.; Hazendonk, P. Validation of the Yen–Mullins Model of Athabasca Oil-Sands Asphaltenes using Solution-State 1H NMR Relaxation and 2D HSQC Spectroscopy. *Energy Fuels* **2013**, *27*, 6528–6537. [CrossRef]

90. Morgan, T.J.; Alvarez-Rodriguez, P.; George, A.; Herod, A.A.; Kandiyoti, R. Characterization of Maya Crude Oil Maltenes and Asphaltenes in Terms of Structural Parameters Calculated from Nuclear Magnetic Resonance (NMR) Spectroscopy and Laser Desorption−Mass Spectroscopy (LD−MS). *Energy Fuels* **2010**, *24*, 3977–3989. [CrossRef]

91. Ok, S.; Mahmoodinia, M.; Rajasekaran, N.; Sabti, M.A.; Lervik, A.; van Erp, T.S.; Cabriolu, R. Molecular Structure and Solubility Determination of Asphaltenes. *Energy Fuels* **2019**, *33*, 8259–8270. [CrossRef]

92. Dickinson, E.M. Structural comparison of petroleum fractions using proton and 13C n.m.r. spectroscopy. *Fuel* **1980**, *59*, 290–294. [CrossRef]

93. Dutta Majumdar, R.; Bake, K.D.; Ratna, Y.; Pomerantz, A.E.; Mullins, O.C.; Gerken, M.; Hazendonk, P. Single-Core PAHs in Petroleum- and Coal-Derived Asphaltenes: Size and Distribution from Solid-State NMR Spectroscopy and Optical Absorption Measurements. *Energy Fuels* **2016**, *30*, 6892–6906. [CrossRef]

94. Dutta Majumdar, R.; Gerken, M.; Hazendonk, P. Solid-State 1H and 13C Nuclear Magnetic Resonance Spectroscopy of Athabasca Oil Sands Asphaltenes: Evidence for Interlocking π-Stacked Nanoaggregates with Intercalated Alkyl Side Chains. *Energy Fuels* **2015**, *29*, 2790–2800. [CrossRef]

95. Andrews, A.B.; Edwards, J.C.; Pomerantz, A.E.; Mullins, O.C.; Nordlund, D.; Norinaga, K. Comparison of Coal-Derived and Petroleum Asphaltenes by 13C Nuclear Magnetic Resonance, DEPT, and XRS. *Energy Fuels* **2011**, *25*, 3068–3076. [CrossRef]

96. Zheng, C.; Zhu, M.; Zhang, D. Characterisation of Asphaltenes Extracted from an Indonesian Oil Sand Using NMR, DEPT and MALDI-TOF. *Energy Procedia* **2015**, *75*, 847–852. [CrossRef]

97. Badu, S.; Pimienta, I.S.O.; Orendt, A.M.; Pugmire, R.J.; Facelli, J.C. Modeling of Asphaltenes: Assessment of Sensitivity of 13C Solid State NMR to Molecular Structure. *Energy Fuels* **2012**, *26*, 2161–2167. [CrossRef]

98. Murphy, P.D.; Gerstein, B.C.; Weinberg, V.L.; Yen, T.F. Determination of chemical functionality in asphaltenes by high-resolution solid-state carbon-13 nuclear magnetic resonance spectrometry. *Anal. Chem.* **1982**, *54*, 522–525. [CrossRef]

99. Morozov, E.V.; Martyanov, O.N. Reversibility of Asphaltene Aggregation As Revealed by Magnetic Resonance Imaging in Situ. *Energy Fuels* **2017**, *31*, 10639–10647. [CrossRef]

100. Morozov, E.V.; Martyanov, O.N. Probing Flocculant-Induced Asphaltene Precipitation via NMR Imaging: From Model Toluene-Asphaltene Systems to Natural Crude Oils. *Appl. Magn. Reson.* **2016**, *47*, 223–235. [CrossRef]

101. Gabrienko, A.A.; Morozov, E.V.; Subramani, V.; Martyanov, O.N.; Kazarian, S.G. Chemical Visualization of Asphaltenes Aggregation Processes Studied in Situ with ATR-FTIR Spectroscopic Imaging and NMR Imaging. *J. Phys. Chem. C* **2015**, *119*, 2646–2660. [CrossRef]

102. Trejo, F.; Ancheyta, J. Characterization of Asphaltene Fractions from Hydrotreated Maya Crude Oil. *Ind. Eng. Chem. Res.* **2007**, *46*, 7571–7579. [CrossRef]

103. Kharrat, A.M. Characterization of Canadian Heavy Oils Using Sequential Extraction Approach. *Energy Fuels* **2009**, *23*, 828–834. [CrossRef]

104. Sadeghi, K.M.; Sadeghi, M.-A.; Wu, W.H.; Yen, T.F. Fractionation of various heavy oils and bitumen for characterization based on polarity. *Fuel* **1989**, *68*, 782–787. [CrossRef]

105. Selucky, M.L.; Kim, S.S.; Skinner, F.; Strausz, O.P. Structure-Related Properties of Athabasca Asphaltenes and Resins as Indicated by Chromatographic Separation. In *Chemistry of Asphaltenes*; American Chemical Society: Washington, DC, USA, 1982; Volume 195, pp. 83–118.

106. Boduszyński, M.; Chadha, B.R.; Szkuta-Pochopień, T. Investigations on Romashkino asphaltic bitumen. 3. Fractionation of asphaltenes using ion-exchange chromatography. *Fuel* **1977**, *56*, 432–436. [CrossRef]

107. Schwager, I.; Kwan, J.T.; Lee, W.C.; Meng, S.; Yen, T.F. Separation and characterization of synthoil asphaltene by gel permeation chromatography and proton nuclear magnetic resonance spectrometry. *Anal. Chem.* **1979**, *51*, 1803–1806. [CrossRef]

108. Carbognani, L. Preparative Subfractionation of Petroleum Resins and Asphaltenes. I. Development of Size Exclusion Separation Methodology. *Pet. Sci. Technol.* **2003**, *21*, 1685–1703. [CrossRef]

109. Haley, G.A. Molecular and unit sheet weights of asphalt fractions separated by gel permeation chromatography. *Anal. Chem.* **1971**, *43*, 371–375. [CrossRef]

110. Gutierrez Sama, S.; Desprez, A.; Krier, G.; Lienemann, C.-P.; Barbier, J.; Lobinski, R.; Barrere-Mangote, C.; Giusti, P.; Bouyssiere, B. Study of the Aggregation of Metal Complexes with Asphaltenes Using Gel Permeation Chromatography Inductively Coupled Plasma High-Resolution Mass Spectrometry. *Energy Fuels* **2016**, *30*, 6907–6912. [CrossRef]

111. Loegel, T.N.; Danielson, N.D.; Borton, D.J.; Hurt, M.R.; Kenttämaa, H.I. Separation of Asphaltenes by Reversed-Phase Liquid Chromatography with Fraction Characterization. *Energy Fuels* **2012**, *26*, 2850–2857. [CrossRef]

112. Morantes, L.R.; Percebom, A.M.; Mejía-Ospino, E. On the molecular basis of aggregation and stability of Colombian asphaltenes and their subfractions. *Fuel* **2019**, *241*, 542–549. [CrossRef]

113. Gawrys, K.L.; Blankenship, G.A.; Kilpatrick, P.K. On the Distribution of Chemical Properties and Aggregation of Solubility Fractions in Asphaltenes. *Energy Fuels* **2006**, *20*, 705–714. [CrossRef]

114. Nalwaya, V.; Tantayakom, V.; Piumsomboon, P.; Fogler, S. Studies on Asphaltenes through Analysis of Polar Fractions. *Ind. Eng. Chem. Res.* **1999**, *38*, 964–972. [CrossRef]

115. Kaminski, T.J.; Fogler, H.S.; Wolf, N.; Wattana, P.; Mairal, A. Classification of Asphaltenes via Fractionation and the Effect of Heteroatom Content on Dissolution Kinetics. *Energy Fuels* **2000**, *14*, 25–30. [CrossRef]

116. Wattana, P.; Fogler, H.S.; Yen, A.; Carmen Garcìa, M.D.; Carbognani, L. Characterization of Polarity-Based Asphaltene Subfractions. *Energy Fuels* **2005**, *19*, 101–110. [CrossRef]

117. Yang, X.; Hamza, H.; Czarnecki, J. Investigation of Subfractions of Athabasca Asphaltenes and Their Role in Emulsion Stability. *Energy Fuels* **2004**, *18*, 770–777. [CrossRef]

118. Schabron, J.F.; Rovani, J.F. On-column precipitation and re-dissolution of asphaltenes in petroleum residua. *Fuel* **2008**, *87*, 165–176. [CrossRef]

119. Rogel, E.; Ovalles, C.; Moir, M.E.; Schabron, J.F. Determination of Asphaltenes in Crude Oil and Petroleum Products by the on Column Precipitation Method. *Energy Fuels* **2009**, *23*, 4515–4521. [CrossRef]

120. Rogel, E.; Ovalles, C.; Vien, J.; Moir, M. Asphaltene content by the in-line filtration method. *Fuel* **2016**, *171*, 203–209. [CrossRef]

121. Fenistein, D.; Barré, L. Experimental measurement of the mass distribution of petroleum asphaltene aggregates using ultracentrifugation and small-angle X-ray scattering. *Fuel* **2001**, *80*, 283–287. [CrossRef]

122. Barré, L.; Simon, S.; Palermo, T. Solution Properties of Asphaltenes. *Langmuir* **2008**, *24*, 3709–3717. [CrossRef]

123. Herzog, P.; Tchoubar, D.; Espinat, D. Macrostructure of asphaltene dispersions by small-angle X-ray scattering. *Fuel* **1988**, *67*, 245–250. [CrossRef]

124. Hoepfner, M.P.; Yang, Y. Ultra-Small-Angle X-Ray Scattering as a Probe of Petroleum Heterogeneities from the Nano- to the Macroscale. In *Chemistry Solutions to Challenges in the Petroleum Industry*; American Chemical Society: Washington, DC, USA, 2019; Volume 1320, pp. 67–87.

125. Yang, Y.; Chaisoontornyotin, W.; Hoepfner, M.P. Structure of Asphaltenes during Precipitation Investigated by Ultra-Small-Angle X-ray Scattering. *Langmuir* **2018**, *34*, 10371–10380. [CrossRef]

126. Ismail, M.; Yang, Y.; Chaisoontornyotin, W.; Ovalles, C.; Rogel, E.; Moir, M.E.; Hoepfner, M.P. Effect of Chemical Inhibitors on Asphaltene Precipitation and Morphology Using Ultra-Small-Angle X-ray Scattering. *Energy Fuels* **2019**, *33*, 3681–3693. [CrossRef]

127. Bouhadda, Y.; Bormann, D.; Sheu, E.; Bendedouch, D.; Krallafa, A.; Daaou, M. Characterization of Algerian Hassi-Messaoud asphaltene structure using Raman spectrometry and X-ray diffraction. *Fuel* **2007**, *86*, 1855–1864. [CrossRef]

128. Andersen, S.I.; Jensen, J.O.; Speight, J.G. X-ray Diffraction of Subfractions of Petroleum Asphaltenes. *Energy Fuels* **2005**, *19*, 2371–2377. [CrossRef]

129. Guiliano, M.; Boukir, A.; Doumenq, P.; Mille, G.; Crampon, C.; Badens, E.; Charbit, G. Supercritical Fluid Extraction of Bal 150 Crude Oil Asphaltenes. *Energy Fuels* **2000**, *14*, 89–94. [CrossRef]

130. Zhang, L.; Xu, Z.; Quan, S.; Sun, X.; Na, Z.; Zhang, Y.; Chung, K.H.; Xu, C.; Zhao, S. Molecular Characterization of Polar Heteroatom Species in Venezuela Orinoco Petroleum Vacuum Residue and Its Supercritical Fluid Extraction Subfractions. *Energy Fuels* **2012**, *26*, 5795–5803. [CrossRef]

131. Zheng, F.; Chung, W.; Palmisano, E.; Dong, D.; Shi, Q.; Xu, Z.; Chung, K.H. Molecular characterization of polar heteroatom species in oilsands bitumen-derived vacuum residue fractions by Fourier transform ion cyclotron resonance mass spectrometry. *Pet. Sci.* **2019**, *16*, 1196–1207. [CrossRef]

132. Marques, J.; Merdrignac, I.; Baudot, A.; Barré, L.; Guillaume, D.; Espinat, D.; Brunet, S. Asphaltenes size polydispersity reduction by nano-and ultrafiltration separation methods–comparison with the flocculation method. *Oil Gas Sci. Technol. Rev. L'IFP* **2008**, *63*, 139–149. [CrossRef]

133. Marques, J.; Guillaume, D.; Merdrignac, I.; Espinat, D.; Barré, L.; Brunet, S. Asphaltene cross-flow membrane ultrafiltration on a preparative scale and feedstock reconstitution method. *Oil Gas Sci. Technol. Rev. L'IFP* **2009**, *64*, 795–806. [CrossRef]

134. Subramanian, S.; Simon, S.; Gao, B.; Sjöblom, J. Asphaltene fractionation based on adsorption onto calcium carbonate: Part 1. Characterization of sub-fractions and QCM-D measurements. *Colloids Surf. A Physicochem. Eng. Asp.* **2016**, *495*, 136–148. [CrossRef]

135. Subramanian, S.; Sørland, G.H.; Simon, S.; Xu, Z.; Sjöblom, J. Asphaltene fractionation based on adsorption onto calcium carbonate: Part 2. Self-association and aggregation properties. *Colloids Surf. A Physicochem. Eng. Asp.* **2017**, *514*, 79–90. [CrossRef]

136. Ruwoldt, J.; Subramanian, S.; Simon, S.; Oschmann, H.; Sjöblom, J. Asphaltene fractionation based on adsorption onto calcium carbonate: Part 3. Effect of asphaltenes on wax crystallization. *Colloids Surf. A Physicochem. Eng. Asp.* **2018**, *554*, 129–141. [CrossRef]

137. Taheri-Shakib, J.; Rajabi-Kochi, M.; Kazemzadeh, E.; Naderi, H.; Salimidelshad, Y.; Esfahani, M.R. A comprehensive study of asphaltene fractionation based on adsorption onto calcite, dolomite and sandstone. *J. Pet. Sci. Eng.* **2018**, *171*, 863–878. [CrossRef]

138. Taheri-Shakib, J.; Hosseini, S.A.; Kazemzadeh, E.; Keshavarz, V.; Rajabi-Kochi, M.; Naderi, H. Experimental and mathematical model evaluation of asphaltene fractionation based on adsorption in porous media: Dolomite reservoir rock. *Fuel* **2019**, *245*, 570–585. [CrossRef]

139. Taheri-Shakib, J.; Keshavarz, V.; Kazemzadeh, E.; Hosseini, S.A.; Rajabi-Kochi, M.; Salimidelshad, Y.; Naderi, H.; Bakhtiari, H.A. Experimental and mathematical model evaluation of asphaltene fractionation based on adsorption in porous media: Part 1. calcite reservoir rock. *J. Pet. Sci. Eng.* **2019**, *177*, 24–40. [CrossRef]

140. Fan, S.; Liu, H.; Wang, J.; Chen, H.; Bai, R.; Guo, A.; Chen, K.; Huang, J.; Wang, Z. Microwave-assisted Petroporphyrin Release from Asphaltene Aggregates in Polar Solvents. *Energy Fuels* **2020**, *34*, 2683–2692. [CrossRef]

141. Bunger, J.W.; Li, N.C. *Chemistry of Asphaltenes*; American Chemical Society: Washington, DC, USA, 1981.

142. Hosseini-Dastgerdi, Z.; Tabatabaei-Nejad, S.A.R.; Khodapanah, E.; Sahraei, E. A comprehensive study on mechanism of formation and techniques to diagnose asphaltene structure; molecular and aggregates: A review. *Asia Pac. J. Chem. Eng.* **2015**, *10*, 1–14. [CrossRef]

143. Czogalla, C.-D.; Boberg, F. Sulfur Compounds in Fossil Fuels I. *Sulfur Rep.* **1983**, *3*, 121–161. [CrossRef]

144. Hsu, C.S. *Analytical Advances for Hydrocarbon Research*; Springer Science and Business Media: New York, NY, USA, 2003.

145. Coelho, R.R.; Hovell, I.; Rajagopal, K. Elucidation of the functional sulphur chemical structure in asphaltenes using first principles and deconvolution of mid-infrared vibrational spectra. *Fuel Process. Technol.* **2012**, *97*, 85–92. [CrossRef]

146. George, G.N.; Gorbaty, M.L. Sulfur K-edge x-ray absorption spectroscopy of petroleum asphaltenes and model compounds. *J. Am. Chem. Soc.* **1989**, *111*, 3182–3186. [CrossRef]

147. Waldo, G.S.; Mullins, O.C.; Penner-Hahn, J.E.; Cramer, S.P. Determination of the chemical environment of sulphur in petroleum asphaltenes by X-ray absorption spectroscopy. *Fuel* **1992**, *71*, 53–57. [CrossRef]

148. Bava, Y.B.; Geronés, M.; Giovanetti, L.J.; Andrini, L.; Erben, M.F. Speciation of sulphur in asphaltenes and resins from Argentinian petroleum by using XANES spectroscopy. *Fuel* **2019**, *256*, 115952. [CrossRef]

149. Zhang, L.-L.; Wang, C.-L.; Zhao, Y.-S.; Yang, G.-H.; Su, M.; Yang, C.-H. Speciation and quantification of sulfur compounds in petroleum asphaltenes by derivative XANES spectra. *J. Fuel Chem. Technol.* **2013**, *41*, 1328–1335. [CrossRef]

150. Vargas, V.; Castillo, J.; Ocampo Torres, R.; Bouyssiere, B.; Lienemann, C.-P. Development of a chromatographic methodology for the separation and quantification of V, Ni and S compounds in petroleum products. *Fuel Process. Technol.* **2017**, *162*, 37–44. [CrossRef]

151. Wang, S.; Yang, C.; Xu, C.; Zhao, S.; Shi, Q. Separation and characterization of petroleum asphaltene fractions by ESI FT-ICR MS and UV-vis spectrometer. *Sci. China Chem.* **2013**, *56*, 856–862. [CrossRef]

152. Wang, L.; He, C.; Liu, Y.; Zhao, S.; Zhang, Y.; Xu, C.; Chung, K.; Shi, Q. Effects of experimental conditions on the molecular composition of maltenes and asphaltenes derived from oilsands bitumen: Characterized by negative-ion ESI FT-ICR MS. *Sci. China Chem.* **2013**, *56*, 863–873. [CrossRef]

153. Cho, Y.; Na, J.-G.; Nho, N.-S.; Kim, S.; Kim, S. Application of Saturates, Aromatics, Resins, and Asphaltenes Crude Oil Fractionation for Detailed Chemical Characterization of Heavy Crude Oils by Fourier Transform Ion Cyclotron Resonance Mass Spectrometry Equipped with Atmospheric Pressure Photoionization. *Energy Fuels* **2012**, *26*, 2558–2565. [CrossRef]

154. Qian, K.; Mennito, A.S.; Edwards, K.E.; Ferrughelli, D.T. Observation of vanadyl porphyrins and sulfur-containing vanadyl porphyrins in a petroleum asphaltene by atmospheric pressure photonionization Fourier transform ion cyclotron resonance mass spectrometry. *Rapid Commun. Mass Spectrom.* **2008**, *22*, 2153–2160. [CrossRef]

155. Qian, K.; Rodgers, R.P.; Hendrickson, C.L.; Emmett, M.R.; Marshall, A.G. Reading Chemical Fine Print: Resolution and Identification of 3000 Nitrogen-Containing Aromatic Compounds from a Single Electrospray Ionization Fourier Transform Ion Cyclotron Resonance Mass Spectrum of Heavy Petroleum Crude Oil. *Energy Fuels* **2001**, *15*, 492–498. [CrossRef]

156. Ignasiak, T.; Strausz, O.P.; Montgomery, D.S. Oxygen distribution and hydrogen bonding in Athabasca asphaltene. *Fuel* **1977**, *56*, 359–365. [CrossRef]

157. Zheng, C.; Brunner, M.; Li, H.; Zhang, D.; Atkin, R. Dissolution and suspension of asphaltenes with ionic liquids. *Fuel* **2019**, *238*, 129–138. [CrossRef]

158. Moschopedis, S.E.; Speight, J.G. Oxygen functions in asphaltenes. *Fuel* **1976**, *55*, 334–336. [CrossRef]

159. Chacón-Patiño, M.L.; Smith, D.F.; Hendrickson, C.L.; Marshall, A.G.; Rodgers, R.P. Advances in Asphaltene Petroleomics. Part 4. Compositional Trends of Solubility Subfractions Reveal that Polyfunctional Oxygen-Containing Compounds Drive Asphaltene Chemistry. *Energy Fuels* **2020**, *34*, 3013–3030. [CrossRef]

160. Treibs, A. Chlorophyll- und Häminderivate in bituminösen Gesteinen, Erdölen, Erdwachsen und Asphalten. Ein Beitrag zur Entstehung des Erdöls. *Justus Liebigs Ann. Der Chem.* **1934**, *510*, 42–62. [CrossRef]

161. Treibs, A. Chlorophyll- und Häminderivate in organischen Mineralstoffen. *Angew. Chem.* **1936**, *49*, 682–686. [CrossRef]

162. Dunning, H.N.; Moore, J.W. Porphyrin research and origin of petroleum. *AAPG Bull.* **1957**, *41*, 2403–2412.

163. Senglet, N.; Williams, C.; Faure, D.; Des Courières, T.; Guilard, R. Microheterogeneity study of heavy crude petroleum by u.v.-visible spectroscopy and small angle X-ray scattering. *Fuel* **1990**, *69*, 72–77. [CrossRef]

164. Berthe, C.; Muller, J.; Cagnian, D.; Grinbitt, J.; Bonnelle, J. Characterization of heavy petroleum fractions by IR and UV-visible spectroscopy, ESCA photoelectronic spectroscopy and LAMMA spectroscopy in relation to the vanadium environment. *Collect. Colloq. Semin. (Inst. Fr. Pet.)* **1984**, *40*, 164–168.

165. Goulon, J.; Retournard, A.; Friant, P.; Goulon-Ginet, C.; Berthe, C.; Muller, J.-F.; Poncet, J.-L.; Guilard, R.; Escalier, J.-C.; Neff, B. Structural characterization by X-ray absorption spectroscopy (EXAFS/XANES) of the vanadium chemical environment in Boscan asphaltenes. *J. Chem. Soc. Dalton Trans.* **1984**, 1095–1103. [CrossRef]

166. Poncet, J.; Guilard, R.; Friant, P.; Goulonginet, C.; Goulon, J. Vanadium (IV) porphyrins-synthesis and classification of thiovanadyl and selenovanadyl porphyrins-EXAFS and RPE spectroscopic studies. *Nouv. J. Chim. New J. Chem.* **1984**, *8*, 583–590.

167. Loos, M.; Ascone, I.; Friant, P.; Ruiz-Lopez, M.F.; Goulon, J.; Barbe, J.M.; Senglet, N.; Guilard, R.; Faure, D.; Des Courieres, T. Vanadyl porphyrins: Evidence for self-association and for specific interactions with hydroprocessing catalysts shown from X.A.F.S. and E.S.R. studies. *Catal. Today* **1990**, *7*, 497–513. [CrossRef]

168. Yokota, T.; Scriven, F.; Montgomery, D.S.; Strausz, O.P. Absorption and emission spectra of Athabasca asphaltene in the visible and near ultraviolet regions. *Fuel* **1986**, *65*, 1142–1149. [CrossRef]

169. Antipenko, V.; Zemtseva, L. Multiplicative hindrances in the quantitative analysis of petroleum metal porphyrins. *Pet. Chem.* **1996**, *36*, 31–42.

170. Gallegos, E.J.; Fetzer, J.C.; Carlson, R.M.; Pena, M.M. High-temperature GC/MS characterization of porphyrins and high molecular weight saturated hydrocarbons. *Energy Fuels* **1991**, *5*, 376–381. [CrossRef]

171. Philp, R.P. High temperature gas chromatography for the analysis of fossil fuels: A review. *J. High. Resolut. Chromatogr.* **1994**, *17*, 398–406. [CrossRef]

172. McKenna, A.M.; Purcell, J.M.; Rodgers, R.P.; Marshall, A.G. Identification of Vanadyl Porphyrins, in a Heavy Crude Oil and Raw Asphaltene by Atmospheric Pressure Photoionization Fourier Transform Ion Cyclotron Resonance (FT-ICR) Mass Spectrometry. *Energy Fuels* **2009**, *23*, 2122–2128. [CrossRef]

173. Liao, Z.; Huang, D.; Shi, J. Discovery of Special Predominance of Vanadyl Porphyrin and High Abundance of Di-DPEP in Nonmarine Strata. *Sci. China Chem.* **1990**, *33*, 631–640.

174. Qian, K.; Fredriksen, T.R.; Mennito, A.S.; Zhang, Y.; Harper, M.R.; Merchant, S.; Kushnerick, J.D.; Rytting, B.M.; Kilpatrick, P.K. Evidence of naturally-occurring vanadyl porphyrins containing multiple S and O atoms. *Fuel* **2019**, *239*, 1258–1264. [CrossRef]

175. Zhao, X.; Shi, Q.; Gray, M.R.; Xu, C. New Vanadium Compounds in Venezuela Heavy Crude Oil Detected by Positive-ion Electrospray Ionization Fourier Transform Ion Cyclotron Resonance Mass Spectrometry. *Sci. Rep.* **2014**, *4*, 5373. [CrossRef]

176. Kim, T.; Ryu, J.; Kim, M.-J.; Kim, H.-J.; Shul, Y.-G.; Jeon, Y.; Park, J.-I. Characterization and analysis of vanadium and nickel species in atmospheric residues. *Fuel* **2014**, *117*, 783–791. [CrossRef]

177. Zhang, L.; Zhao, S.; Xu, Z.; Chung, K.H.; Zhao, C.; Zhang, N.; Xu, C.; Shi, Q. Molecular Weight and Aggregation of Heavy Petroleum Fractions Measured by Vapor Pressure Osmometry and a Hindered Stepwise Aggregation Model. *Energy Fuels* **2014**, *28*, 6179–6187. [CrossRef]

178. Yarranton, H.W.; Ortiz, D.P.; Barrera, D.M.; Baydak, E.N.; Barré, L.; Frot, D.; Eyssautier, J.; Zeng, H.; Xu, Z.; Dechaine, G.; et al. On the Size Distribution of Self-Associated Asphaltenes. *Energy Fuels* **2013**, *27*, 5083–5106. [CrossRef]

179. Gray, M.R.; Tykwinski, R.R.; Stryker, J.M.; Tan, X. Supramolecular Assembly Model for Aggregation of Petroleum Asphaltenes. *Energy Fuels* **2011**, *25*, 3125–3134. [CrossRef]

180. Östlund, J.-A.; Nydén, M.; Auflem, I.H.; Sjöblom, J. Interactions between Asphaltenes and Naphthenic Acids. *Energy Fuels* **2003**, *17*, 113–119. [CrossRef]

181. Stoyanov, S.R.; Yin, C.-X.; Gray, M.R.; Stryker, J.M.; Gusarov, S.; Kovalenko, A. Computational and Experimental Study of the Structure, Binding Preferences, and Spectroscopy of Nickel(II) and Vanadyl Porphyrins in Petroleum. *J. Phys. Chem. B* **2010**, *114*, 2180–2188. [CrossRef]

182. Gray, M.R.; Yarranton, H.W. Quantitative Modeling of Formation of Asphaltene Nanoaggregates. *Energy Fuels* **2019**, *33*, 8566–8575. [CrossRef]

183. Buenrostro-Gonzalez, E.; Lira-Galeana, C.; Gil-Villegas, A.; Wu, J. Asphaltene precipitation in crude oils: Theory and experiments. *AIChE J.* **2004**, *50*, 2552–2570. [CrossRef]

184. Hassanvand, M.; Shahsavani, B.; Anooshe, A. Study of temperature effect on asphaltene precipitation by visual and quantitative methods. *J. Pet. Technol. Altern. Fuels* **2012**, *3*, 8–18. [CrossRef]

185. Li, X.; Berg, S.; Castellanos-Diaz, O.; Wiegmann, A.; Verlaan, M. Solvent-dependent recovery characteristic and asphaltene deposition during solvent extraction of heavy oil. *Fuel* **2020**, *263*, 116716. [CrossRef]

186. Alimohammadi, S.; Zendehboudi, S.; James, L. A comprehensive review of asphaltene deposition in petroleum reservoirs: Theory, challenges, and tips. *Fuel* **2019**, *252*, 753–791. [CrossRef]

187. Vazquez, D.; Mansoori, G.A. Identification and measurement of petroleum precipitates. *J. Pet. Sci. Eng.* **2000**, *26*, 49–55. [CrossRef]

188. Mullins, O.C. The Modified Yen Model. *Energy Fuels* **2010**, *24*, 2179–2207. [CrossRef]

189. Maqbool, T.; Srikiratiwong, P.; Fogler, H.S. Effect of Temperature on the Precipitation Kinetics of Asphaltenes. *Energy Fuels* **2011**, *25*, 694–700. [CrossRef]

190. Evdokimov, I.N.; Fesan, A.A.; Losev, A.P. New Answers to the Optical Interrogation of Asphaltenes: Complex States of Primary Aggregates from Steady-State Fluorescence Studies. *Energy Fuels* **2016**, *30*, 8226–8235. [CrossRef]

191. Rashid, Z.; Wilfred, C.D.; Gnanasundaram, N.; Arunagiri, A.; Murugesan, T. A comprehensive review on the recent advances on the petroleum asphaltene aggregation. *J. Pet. Sci. Eng.* **2019**, *176*, 249–268. [CrossRef]

192. Yen, T.F.; Erdman, J.G.; Pollack, S.S. Investigation of the Structure of Petroleum Asphaltenes by X-ray Diffraction. *Anal. Chem.* **1961**, *33*, 1587–1594. [CrossRef]

193. Mack, C. Colloid Chemistry of Asphalts. *J. Phys. Chem.* **1932**, *36*, 2901–2914. [CrossRef]

194. Dickie, J.P.; Yen, T.F. Macrostructures of the asphaltic fractions by various instrumental methods. *Anal. Chem.* **1967**, *39*, 1847–1852. [CrossRef]

195. Mullins, O.C.; Sabbah, H.; Eyssautier, J.; Pomerantz, A.E.; Barré, L.; Andrews, A.B.; Ruiz-Morales, Y.; Mostowfi, F.; McFarlane, R.; Goual, L.; et al. Advances in Asphaltene Science and the Yen–Mullins Model. *Energy Fuels* **2012**, *26*, 3986–4003. [CrossRef]

196. Moncada, J.; Schartung, D.; Stephens, N.; Oh, T.-S.; Carrero, C.A. Determining the flocculation point of asphaltenes combining ultrasound and electrochemical impedance spectroscopy. *Fuel* **2019**, *241*, 870–875. [CrossRef]

197. Fossen, M.; Kallevik, H.; Knudsen, K.D.; Sjöblom, J. Asphaltenes Precipitated by a Two-Step Precipitation Procedure. 2. Physical and Chemical Characteristics. *Energy Fuels* **2011**, *25*, 3552–3567. [CrossRef]

198. Schulze, M.; Lechner, M.P.; Stryker, J.M.; Tykwinski, R.R. Aggregation of asphaltene model compounds using a porphyrin tethered to a carboxylic acid. *Org. Biomol. Chem.* **2015**, *13*, 6984–6991. [CrossRef] [PubMed]

199. Akbarzadeh, K.; Bressler, D.C.; Wang, J.; Gawrys, K.L.; Gray, M.R.; Kilpatrick, P.K.; Yarranton, H.W. Association Behavior of Pyrene Compounds as Models for Asphaltenes. *Energy Fuels* **2005**, *19*, 1268–1271. [CrossRef]

200. Tan, X.; Fenniri, H.; Gray, M.R. Pyrene Derivatives of 2,2′-Bipyridine as Models for Asphaltenes: Synthesis, Characterization, and Supramolecular Organization. *Energy Fuels* **2008**, *22*, 715–720. [CrossRef]

201. Rakotondradany, F.; Fenniri, H.; Rahimi, P.; Gawrys, K.L.; Kilpatrick, P.K.; Gray, M.R. Hexabenzocoronene Model Compounds for Asphaltene Fractions: Synthesis and Characterization. *Energy Fuels* **2006**, *20*, 2439–2447. [CrossRef]

202. Duran, J.A.; Schoeggl, F.F.; Yarranton, H.W. Kinetics of asphaltene precipitation/aggregation from diluted crude oil. *Fuel* **2019**, *255*, 115859. [CrossRef]

203. Headen, T.F.; Boek, E.S.; Jackson, G.; Totton, T.S.; Müller, E.A. Simulation of Asphaltene Aggregation through Molecular Dynamics: Insights and Limitations. *Energy Fuels* **2017**, *31*, 1108–1125. [CrossRef]

204. Rogel, E. Studies on asphaltene aggregation via computational chemistry. *Colloids Surf. A Physicochem. Eng. Asp.* **1995**, *104*, 85–93. [CrossRef]

205. Al-Jarrah, M.M.F.; Al-Dujaili, A.H. Chatacterizntian of some iraqi asphalts. II. new findings on the physical nature of asphaltenes. *Fuel Sci. Technol. Int.* **1989**, *7*, 69–88. [CrossRef]

206. Munoz, G.; Gunessee, B.K.; Bégué, D.; Bouyssiere, B.; Baraille, I.; Vallverdu, G.; Santos Silva, H. Redox activity of nickel and vanadium porphyrins: A possible mechanism behind petroleum genesis and maturation? *RSC Adv.* **2019**, *9*, 9509–9516. [CrossRef]

207. Da Costa, L.M.; Stoyanov, S.R.; Gusarov, S.; Tan, X.; Gray, M.R.; Stryker, J.M.; Tykwinski, R.; de Carneiro, M.J.W.; Seidl, P.R.; Kovalenko, A. Density Functional Theory Investigation of the Contributions of π–π Stacking and Hydrogen-Bonding Interactions to the Aggregation of Model Asphaltene Compounds. *Energy Fuels* **2012**, *26*, 2727–2735. [CrossRef]

208. Waters, M.L. Aromatic Interactions. *Acc. Chem. Res.* **2013**, *46*, 873. [CrossRef] [PubMed]

209. Sedghi, M.; Goual, L.; Welch, W.; Kubelka, J. Effect of Asphaltene Structure on Association and Aggregation Using Molecular Dynamics. *J. Phys. Chem. B* **2013**, *117*, 5765–5776. [CrossRef] [PubMed]

210. Santos Silva, H.; Alfarra, A.; Vallverdu, G.; Bégué, D.; Bouyssiere, B.; Baraille, I. Sensitivity of Asphaltene Aggregation toward the Molecular Architecture under Desalting Thermodynamic Conditions. *Energy Fuels* **2018**, *32*, 2681–2692. [CrossRef]

211. Santos Silva, H.; Alfarra, A.; Vallverdu, G.; Bégué, D.; Bouyssiere, B.; Baraille, I. Asphaltene aggregation studied by molecular dynamics simulations: Role of the molecular architecture and solvents on the supramolecular or colloidal behavior. *Pet. Sci.* **2019**, *16*, 669–684. [CrossRef]

212. Silva, H.S.; Sodero, A.C.R.; Bouyssiere, B.; Carrier, H.; Korb, J.-P.; Alfarra, A.; Vallverdu, G.; Bégué, D.; Baraille, I. Molecular Dynamics Study of Nanoaggregation in Asphaltene Mixtures: Effects of the N, O, and S Heteroatoms. *Energy Fuels* **2016**, *30*, 5656–5664. [CrossRef]

213. Santos Silva, H.; Alfarra, A.; Vallverdu, G.; Bégué, D.; Bouyssiere, B.; Baraille, I. Impact of H-Bonds and Porphyrins on Asphaltene Aggregation as Revealed by Molecular Dynamics Simulations. *Energy Fuels* **2018**, *32*, 11153–11164. [CrossRef]

214. Santos Silva, H.; Sodero, A.C.R.; Korb, J.-P.; Alfarra, A.; Giusti, P.; Vallverdu, G.; Bégué, D.; Baraille, I.; Bouyssiere, B. The role of metalloporphyrins on the physical-chemical properties of petroleum fluids. *Fuel* **2017**, *188*, 374–381. [CrossRef]

215. Silva, H.S.; Alfarra, A.; Vallverdu, G.; Bégué, D.; Bouyssiere, B.; Baraille, I. Role of the porphyrins and demulsifiers in the aggregation process of asphaltenes at water/oil interfaces under desalting conditions: A molecular dynamics study. *Pet. Sci.* **2020**, *17*, 797–810. [CrossRef]

216. Giusti, P.; Bouyssiere, B.; Carrier, H.; Afonso, C. 18th International Conference on Petroleum Phase Behavior and Fouling. *Energy Fuels* **2018**, *32*, 2641. [CrossRef]

Publisher's Note: MDPI stays neutral with regard to jurisdictional claims in published maps and institutional affiliations.